GRAVITATIONAL LENSING

23 - STRONG LENSING APPLICATIONS
WEAK LENSING BY GALAXY CLUSTERS

Massimo Meneghetti
AA 2017-2018

COSMOGRAPHY WITH TIME DELAYS

Treu & Marshall, 2016

Time delay distance $\propto \dfrac{1}{H_0}$

Distances encode information on additional cosmological parameters!

$$D_{\Delta t}(z_{\rm d}, z_{\rm s}) = (1 + z_{\rm d})\frac{D_{\rm d} D_{\rm s}}{D_{\rm ds}}$$

$$\tau(\boldsymbol{\theta}) = \frac{D_{\Delta \rm t}}{c} \cdot \Phi(\boldsymbol{\theta}, \boldsymbol{\beta}),$$

$$\text{where } \Phi(\boldsymbol{\theta}) = \frac{1}{2}(\boldsymbol{\theta} - \boldsymbol{\beta})^2 - \psi(\boldsymbol{\theta}).$$

From the lens mass model

- Needed ingredients:
  - Time delays
  - lens mass model

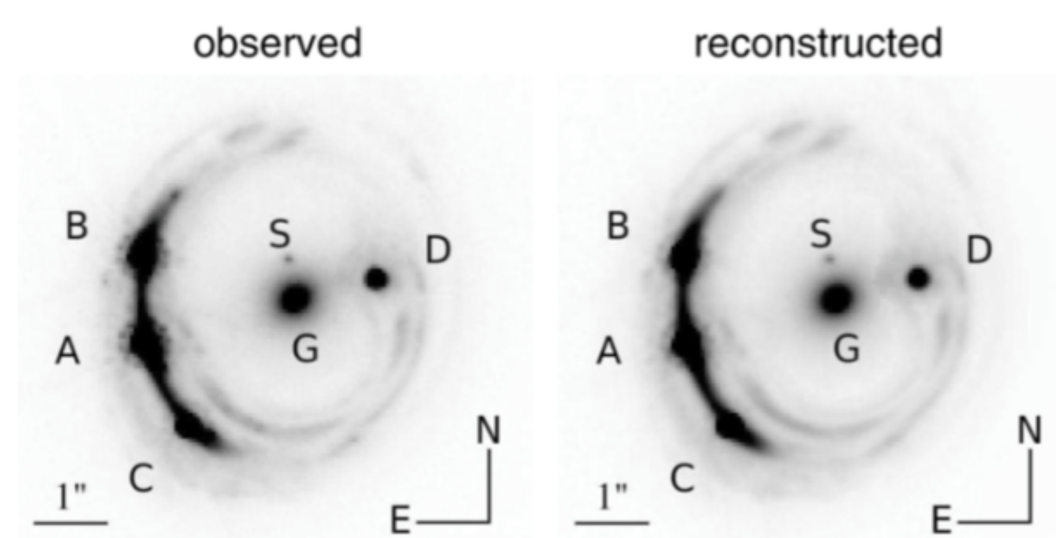

RXJ1131

THE HUBBLE CONSTANT FROM TIME DELAYS

ON THE POSSIBILITY OF DETERMINING HUBBLE'S PARAMETER AND THE MASSES OF GALAXIES FROM THE GRAVITATIONAL LENS EFFECT*

Sjur Refsdal

(Communicated by H. Bondi)

(Received 1964 January 27)

Summary

The gravitational lens effect is applied to a supernova lying far behind and close to the line of sight through a distant galaxy. The light from the supernova may follow two different paths to the observer, and the difference Δt in the time of light travel for these two paths can amount to a couple of months or more, and may be measurable. It is shown that Hubble's parameter and the mass of the galaxy can be expressed by Δt, the red-shifts of the supernova and the galaxy, the luminosities of the supernova "images" and the angle between them. The possibility of observing the phenomenon is discussed.

---

1. *Introduction.*—In 1937 Zwicky suggested that a galaxy, due to the gravitational deflection of light, may act as a gravitational lens. He considered the case of a galaxy *A* lying far behind and close to the line of sight through a distant galaxy *B*. If the line of sight through the centre of *B* goes through *A*, the "image" of *A* will be a ring around *B*, otherwise two separated "images" appear, on opposite sides of *B*. The phenomenon has later been discussed by Zwicky (1957) and Klimov (1963), and they both conclude that the possibility of observing the phenomenon should be good. In the present paper the case of a supernova

TABLE 2

HUBBLE CONSTANT FROM EACH LENS SYSTEM

Lens Name	h (1 σ Range)
B0218+357	0.21 (. . .)
HE 0435−1223	1.02 (0.70–1.39)
RX J0911+0551	0.96 (0.75–1.21)
SBS 0909+532	0.84 (0.47–)
FBQ 0951+2635	0.67 (0.56–0.81)
Q0957+561	0.99 (0.82–1.17)
HE 1104−1805	1.04 (0.92–1.22)
PG 1115+080	0.66 (0.49–0.84)
RX J1131−1231	0.79 (0.59–1.03)
B1422+231	0.16 (–0.36)
SBS 1520+530	0.53 (0.46–0.61)
B1600+434	0.65 (0.54–0.77)
B1608+656	0.89 (0.77–1.20)
SDSS J1650+4251	0.53 (0.44–0.63)
PKS 1830−211	0.88 (0.58–)
HE 2149−2745	0.69 (0.57–0.82)
All	0.70 (0.68–0.73)

NOTE.—The Hubble constant and its error are estimated from the effective χ^2.

Oguri et al. 2007

CURRENT MEASUREMENTS OF TIME DELAYS

Enormous progress in the quality of the light curves since the first measurements thanks to dedicated networks of telescopes. For example: the COSMOGRAIL project measured time delays with precision <4% for 5 lenses

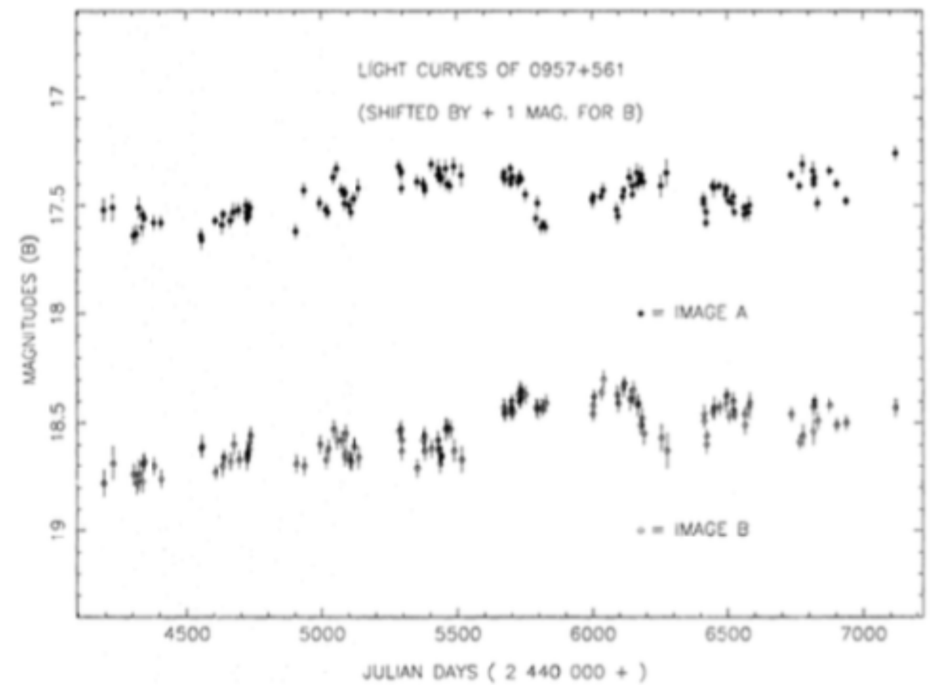

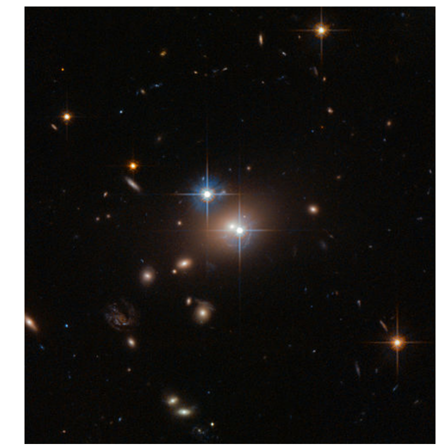

0957+561

Vanderriest et al. 1989

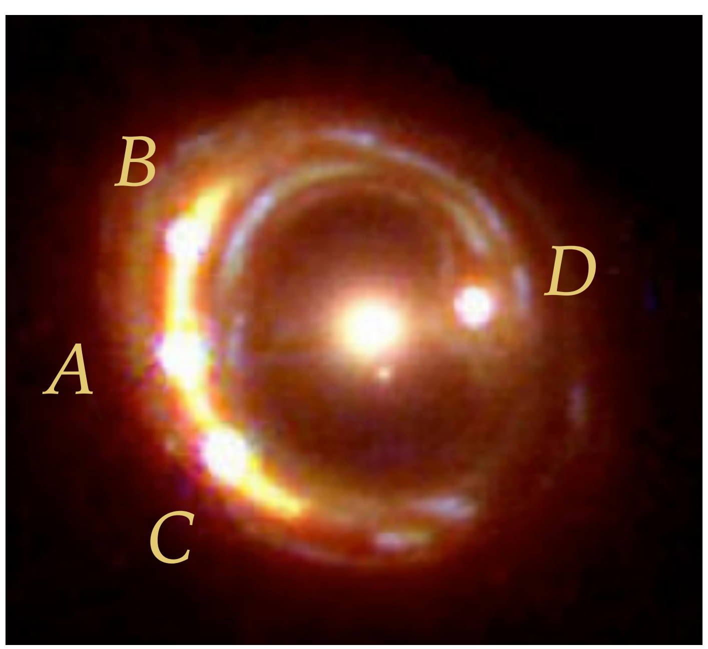

RXJ1131

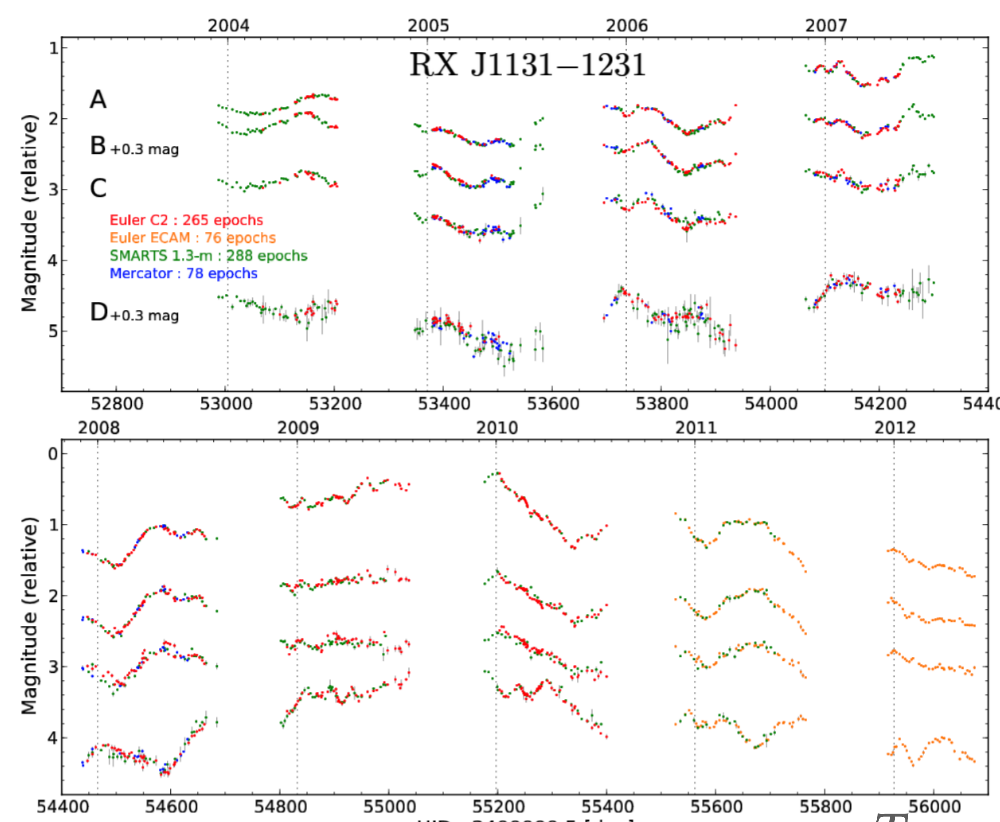

Tewes et al. 2013b

RESULTS FROM THE HOLICOW COLLABORATION

- focussing on the lenses with the best constrained time delays
- recently published results based on three multiply imaged QSOs
- they measure $H_0 = 71.9^{+2.4}_{-3.0}$ km/s/Mpc in a LCDM cosmology
- results are in agreement with cepheids and SNe (SH0ES), but in tension with the recent CMB predictions

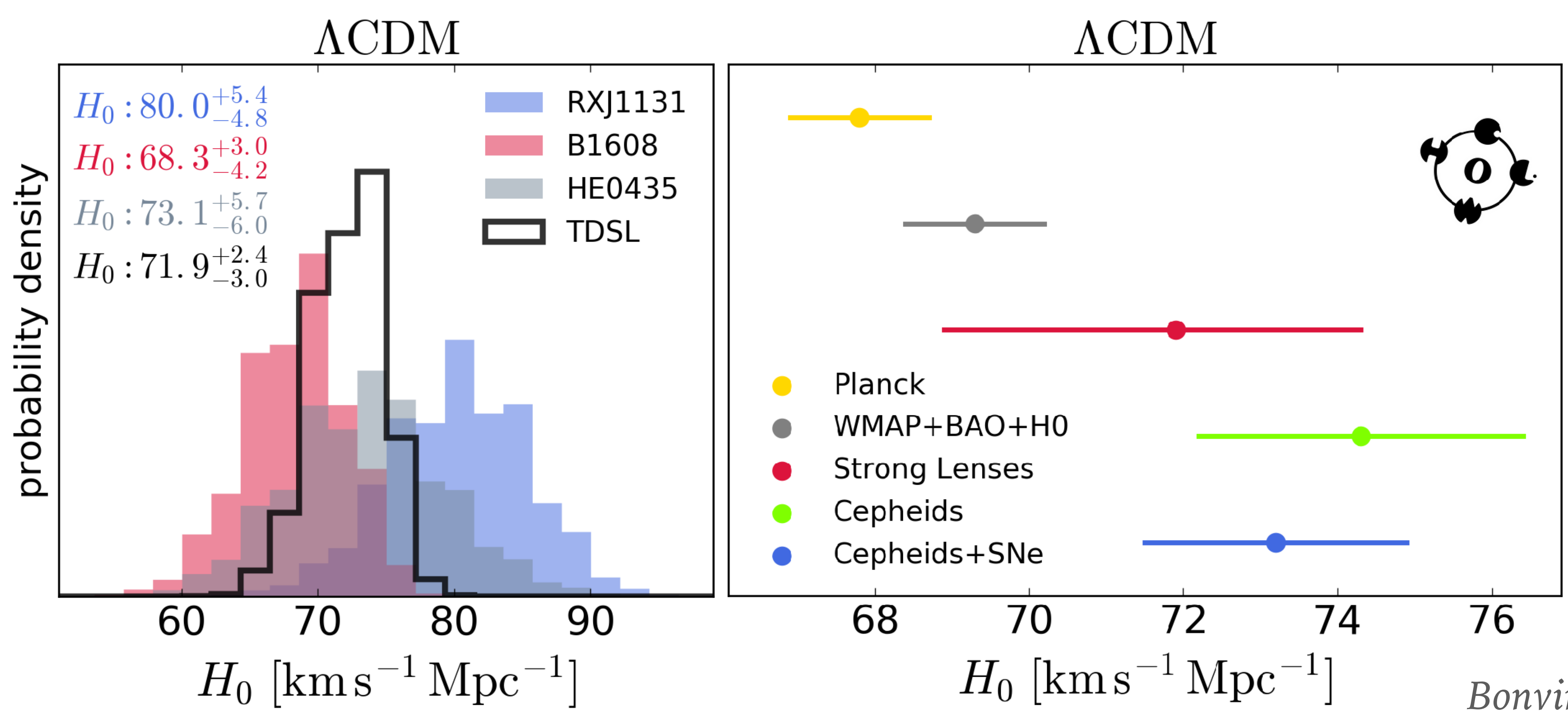

Bonvin et al. 2017

COSMOGRAPHY WITH SOURCES AT MULTIPLE REDSHIFTS

- Even if time delay measurements are not available, the sensitivity to cosmology remains in the astrometric constraints
- With only one lensed source, the distance ratio is degenerate with the mass distribution
- With constraints from multiple sources, one can try to break the degeneracy by measuring the so called "family ratio"
- This technique could be used in the case of e.g. compound lenses, but also in galaxy clusters, where it is easier to observe lensing of many sources

$$\vec{\beta} = \vec{\theta} - \frac{D_{LS}}{D_S}\hat{\vec{\alpha}}(\vec{\theta})$$

depends on cosmology

depends on the mass distr.

$$\Xi_{S1,S2}(\vec{\pi}) = \frac{D_{LS,1}(\vec{\pi})D_{S,2}(\vec{\pi})}{D_{LS,2}(\vec{\pi})D_{S,1}(\vec{\pi})}$$

COSMOGRAPHY: GALAXY CLUSTERS

Mass model with 3 PIEMD potentials; 58 cluster galaxies
Bayesian optimization: 32 constraints, 21 free parameters;
RMS = 0.6 arcsec; 28 multiple images from 12 sources with
spec z, flat Universe prior

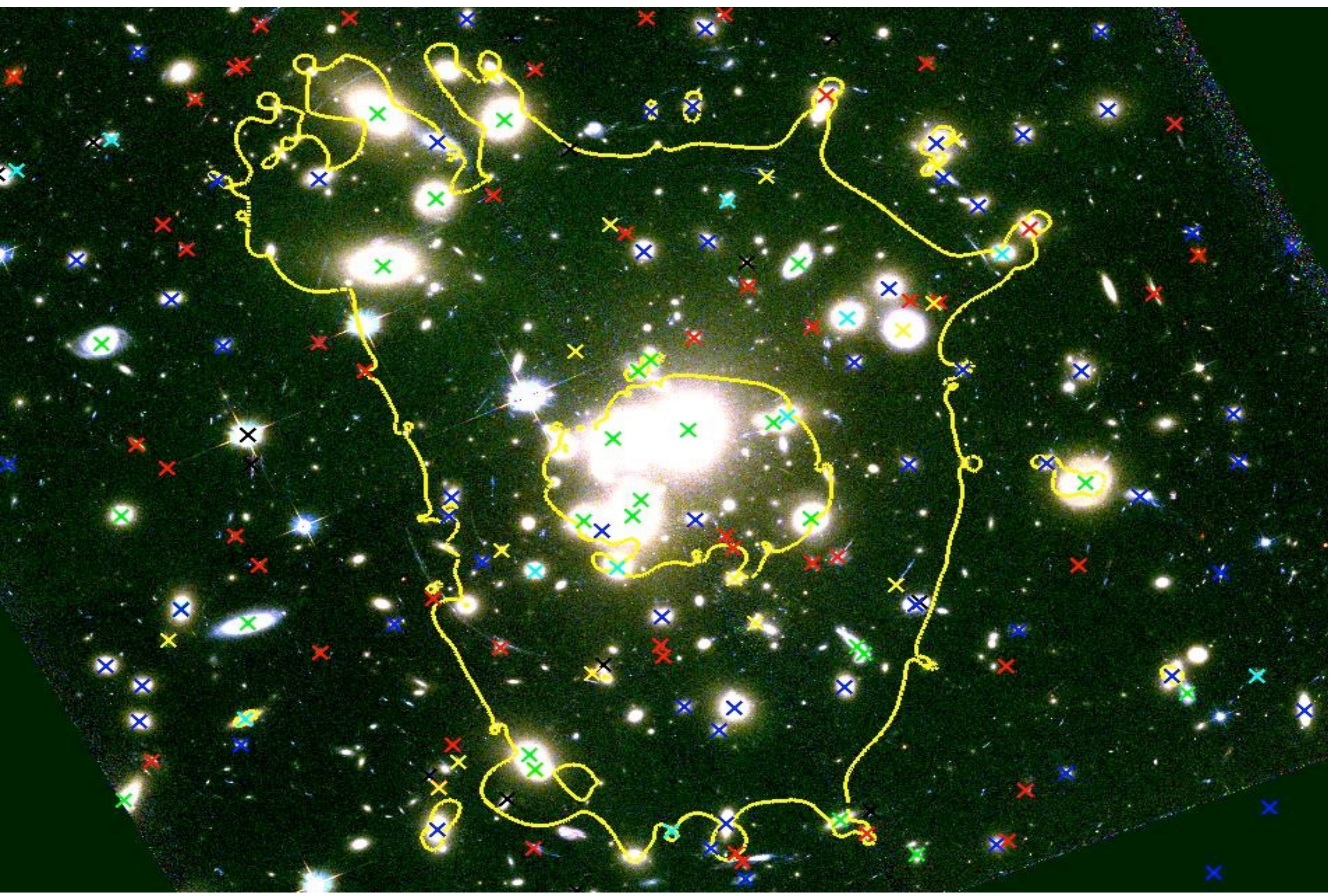

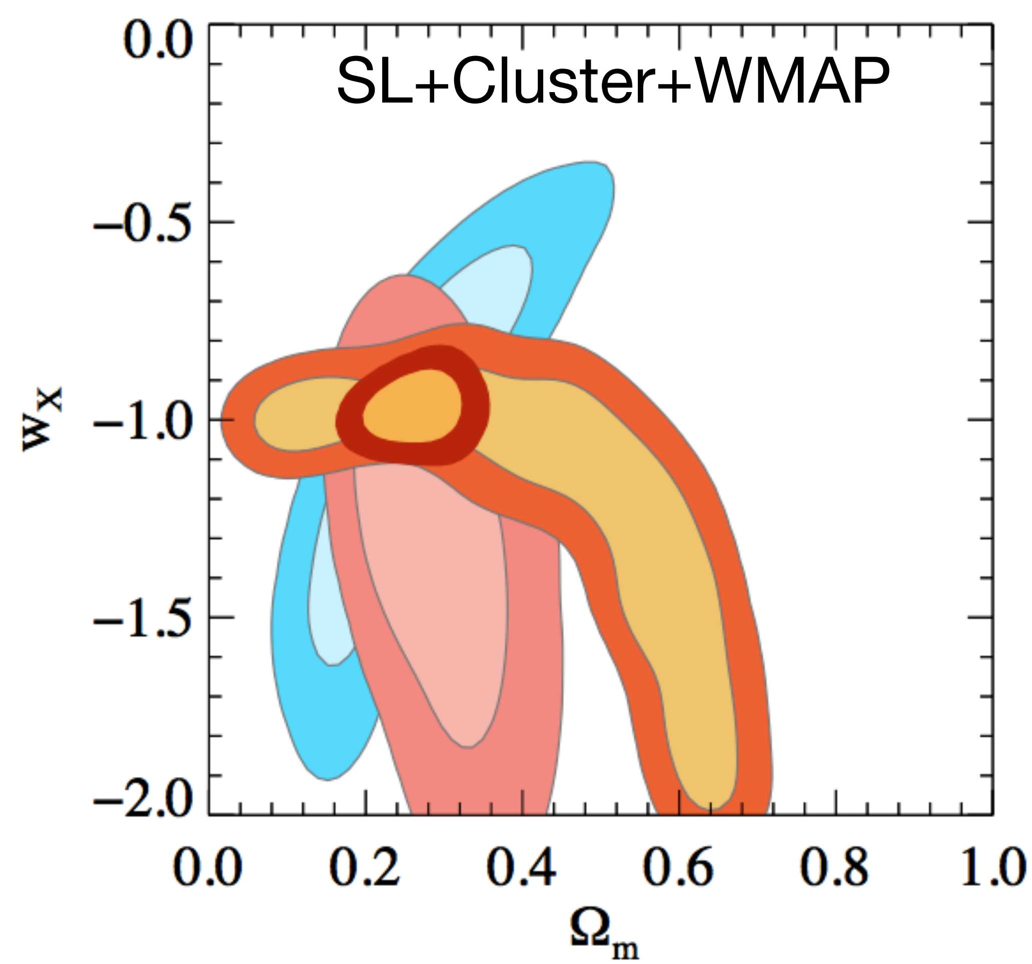

D'Aloisio & Natarajan 10; Jullo & Kneib 09: Jullo+ 10

SN REFSDAL IN MACS 1149

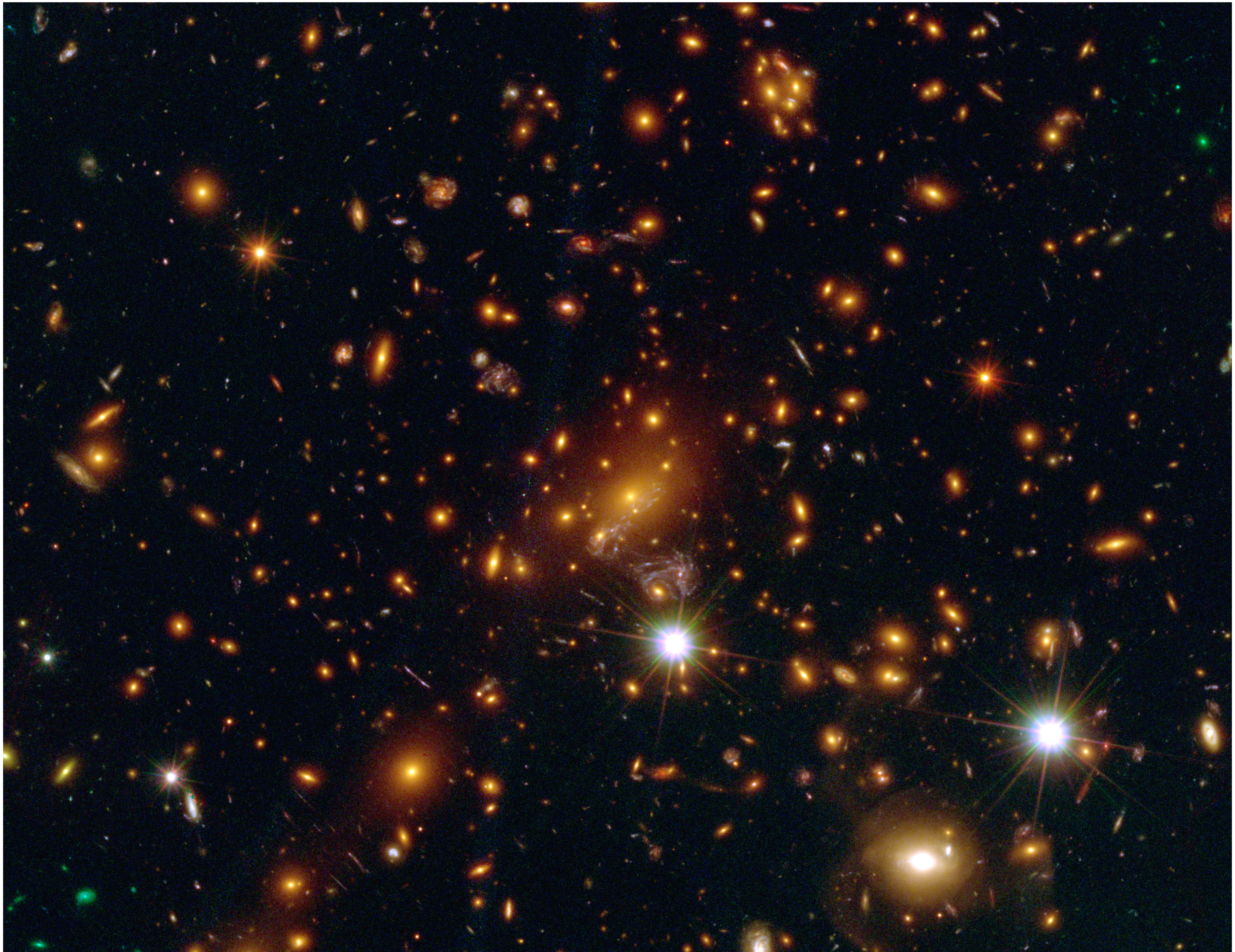

SN REFSDAL IN MACS 1149

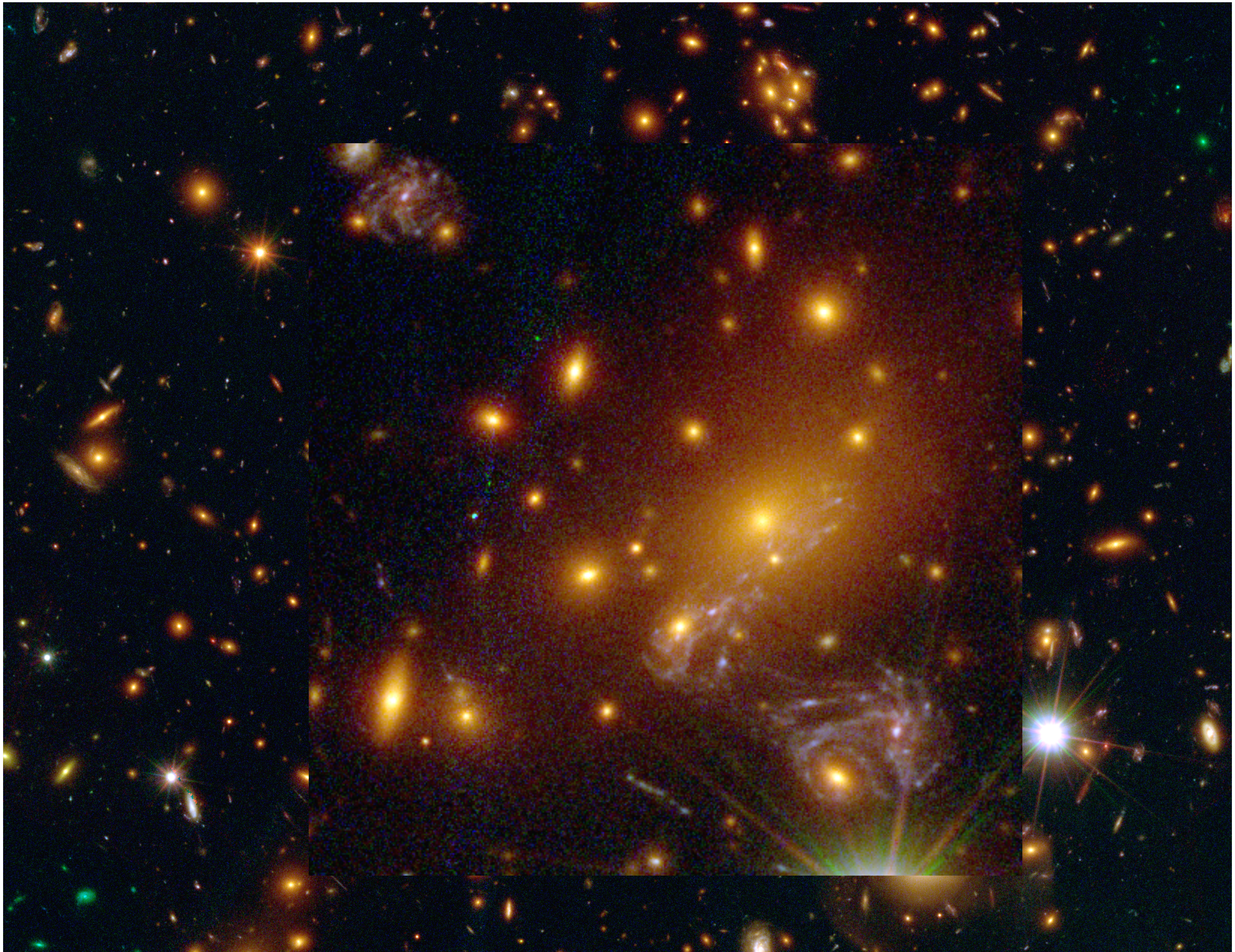

SN REFSDAL IN MACS 1149

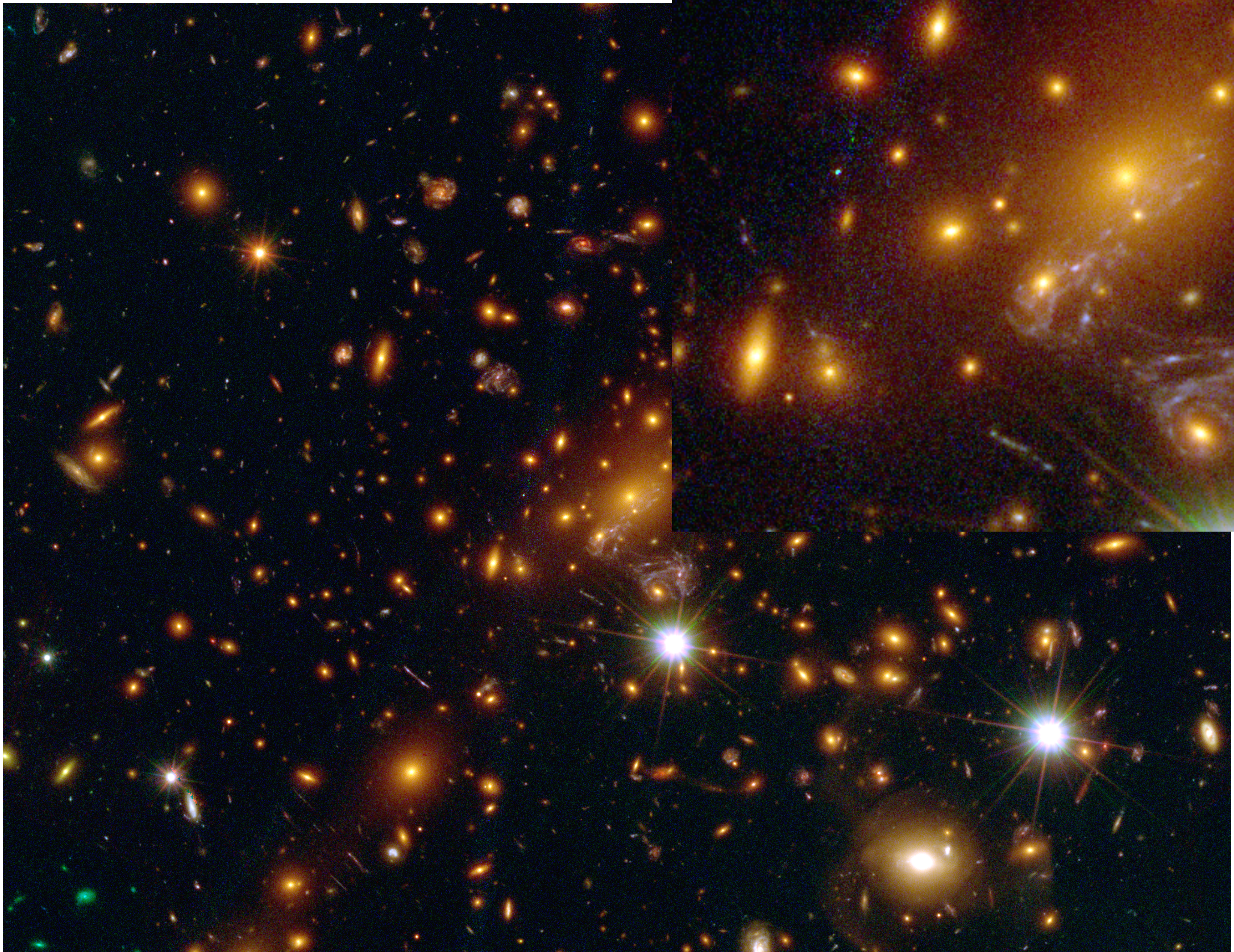

SN REFSDAL IN MACS 1149

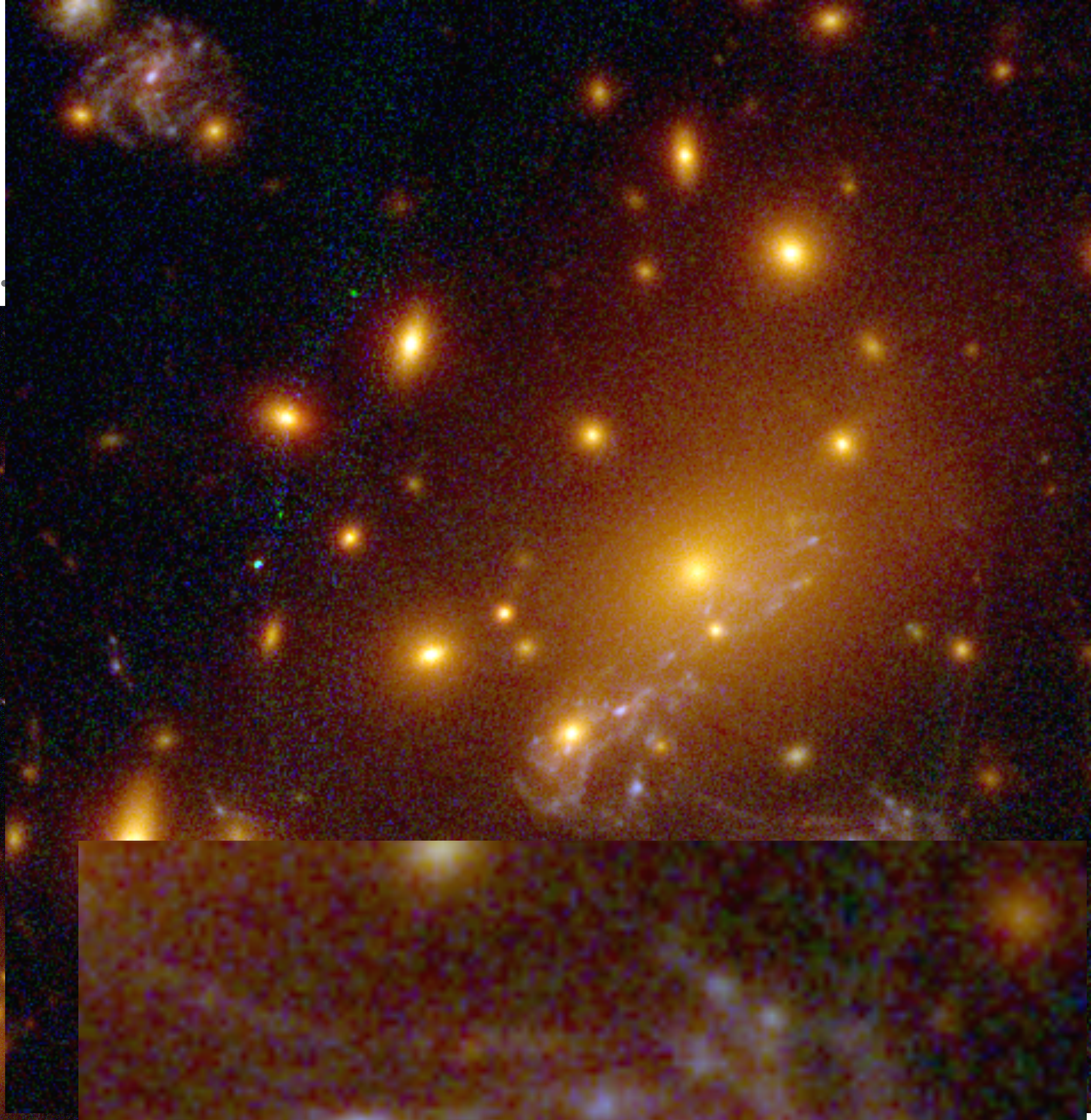

SN REFSDAL IN MACS 1149

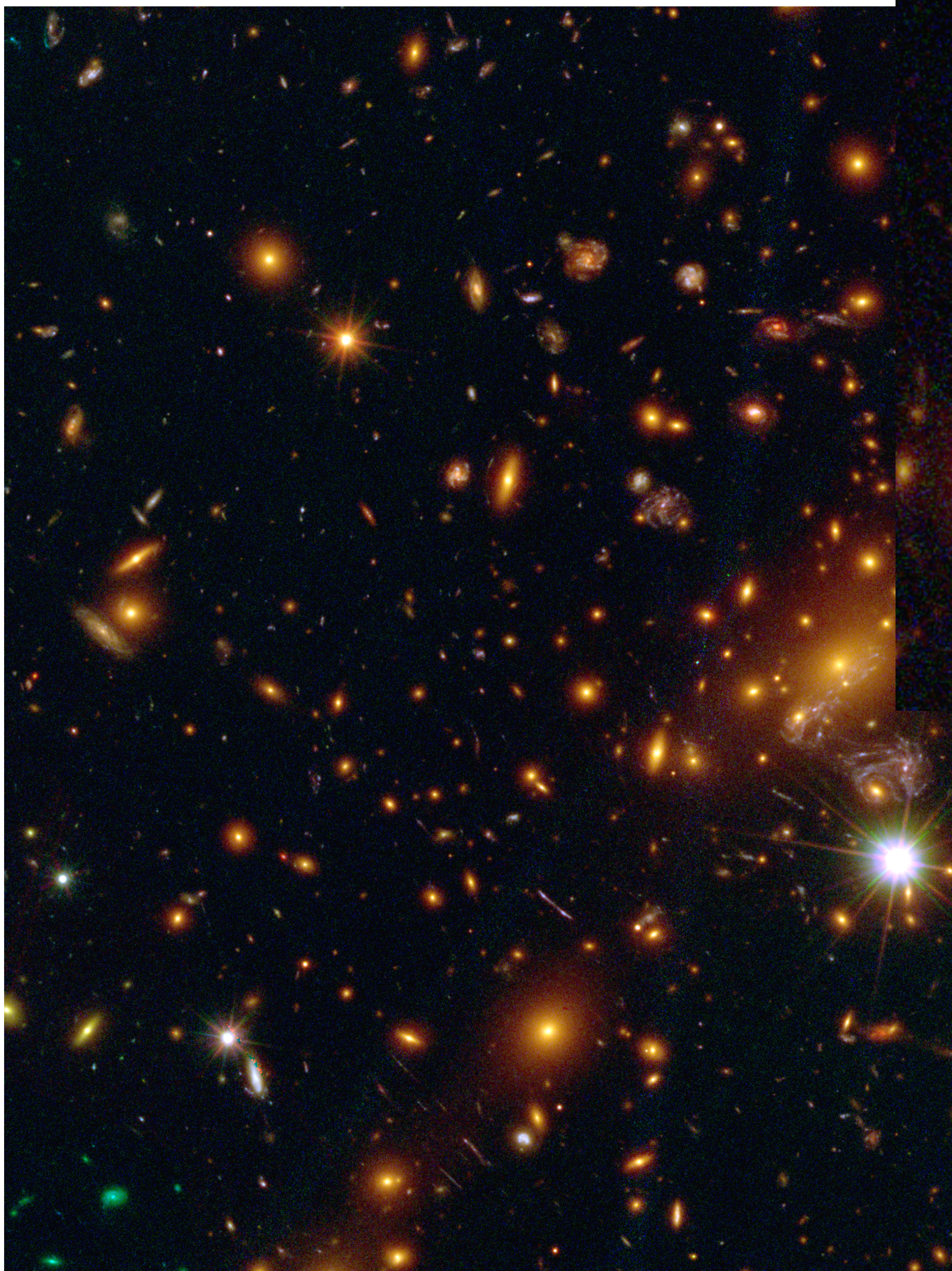

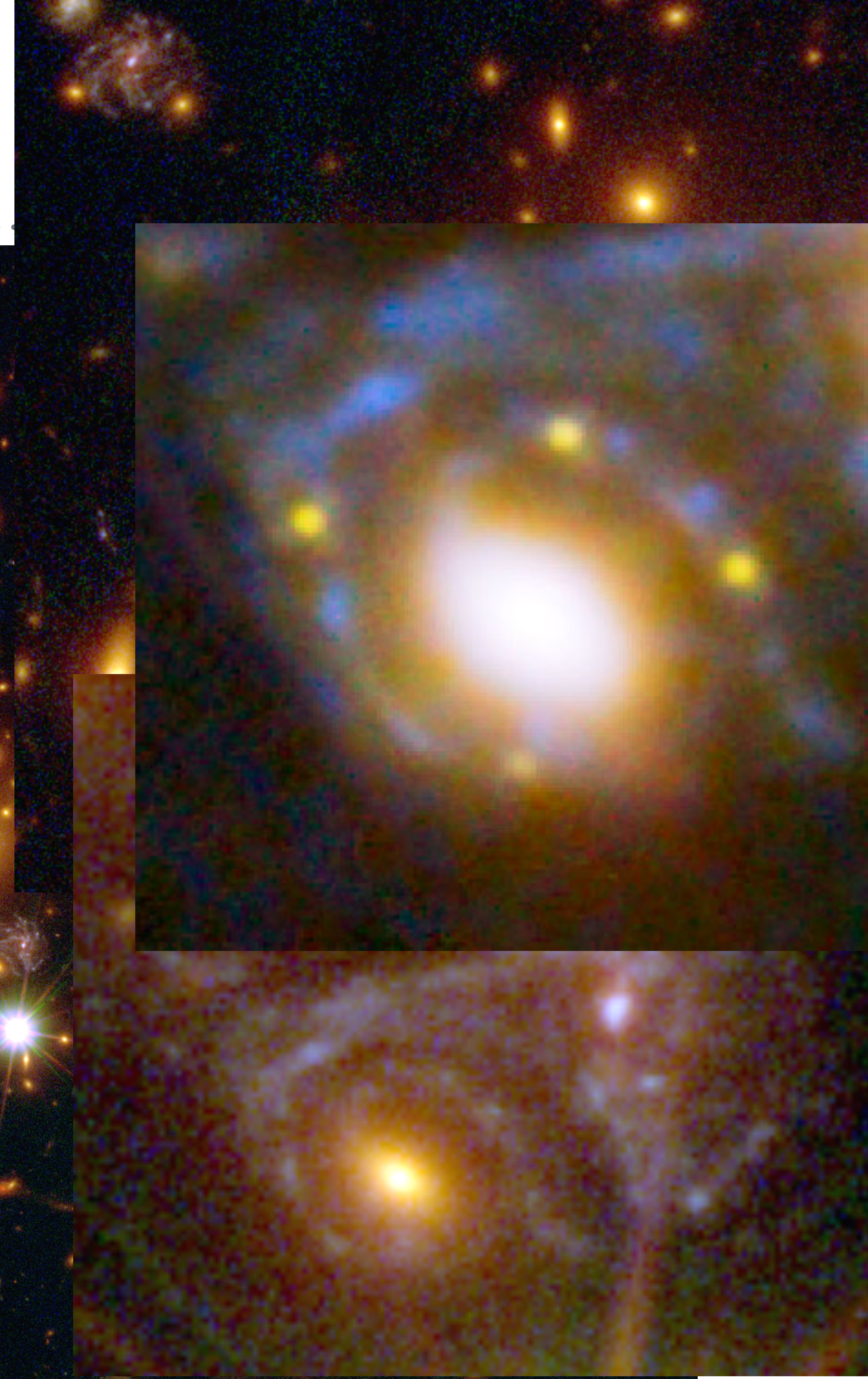

SN REFSDAL IN MACS 1149

Nov. 2014 (Kelly et al.)

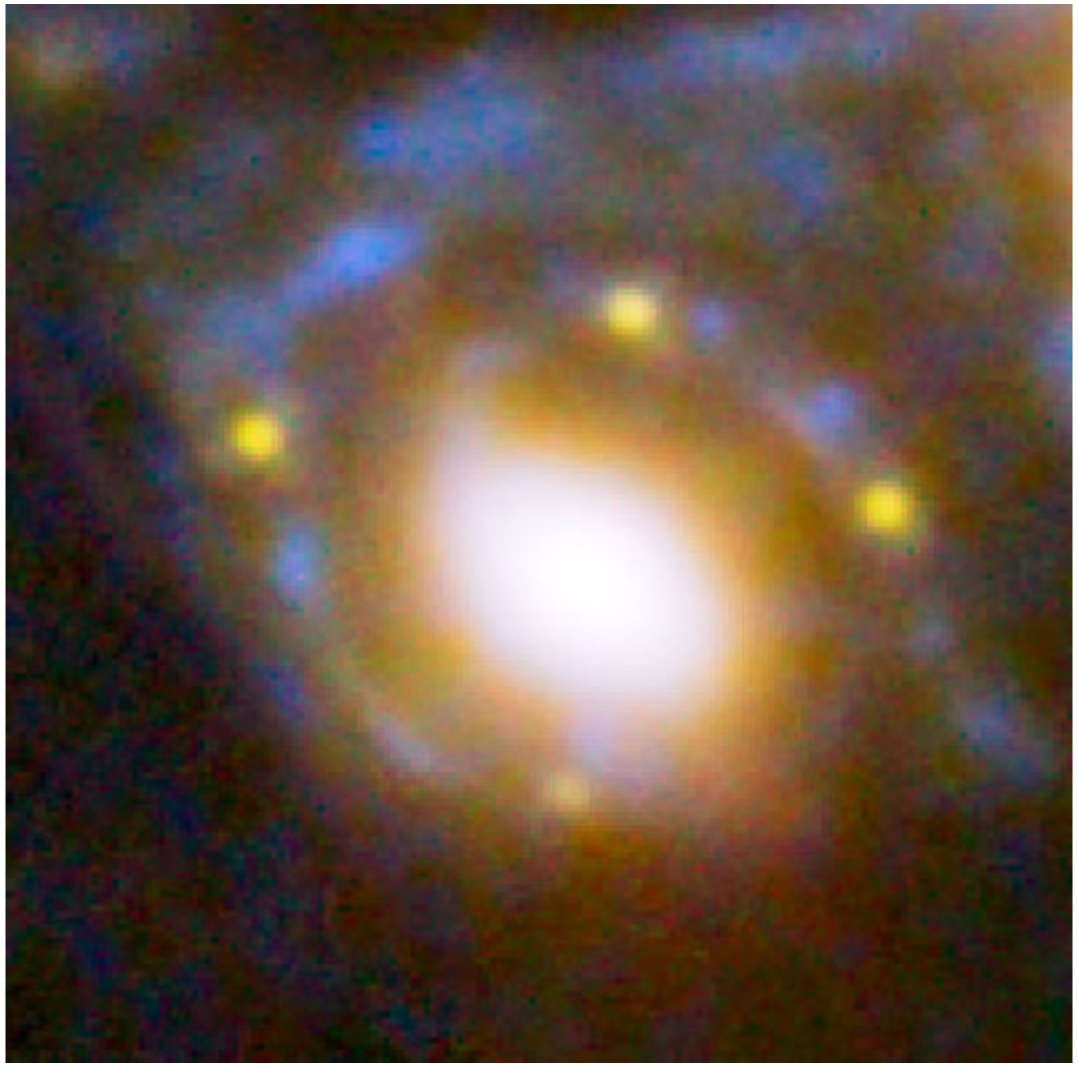

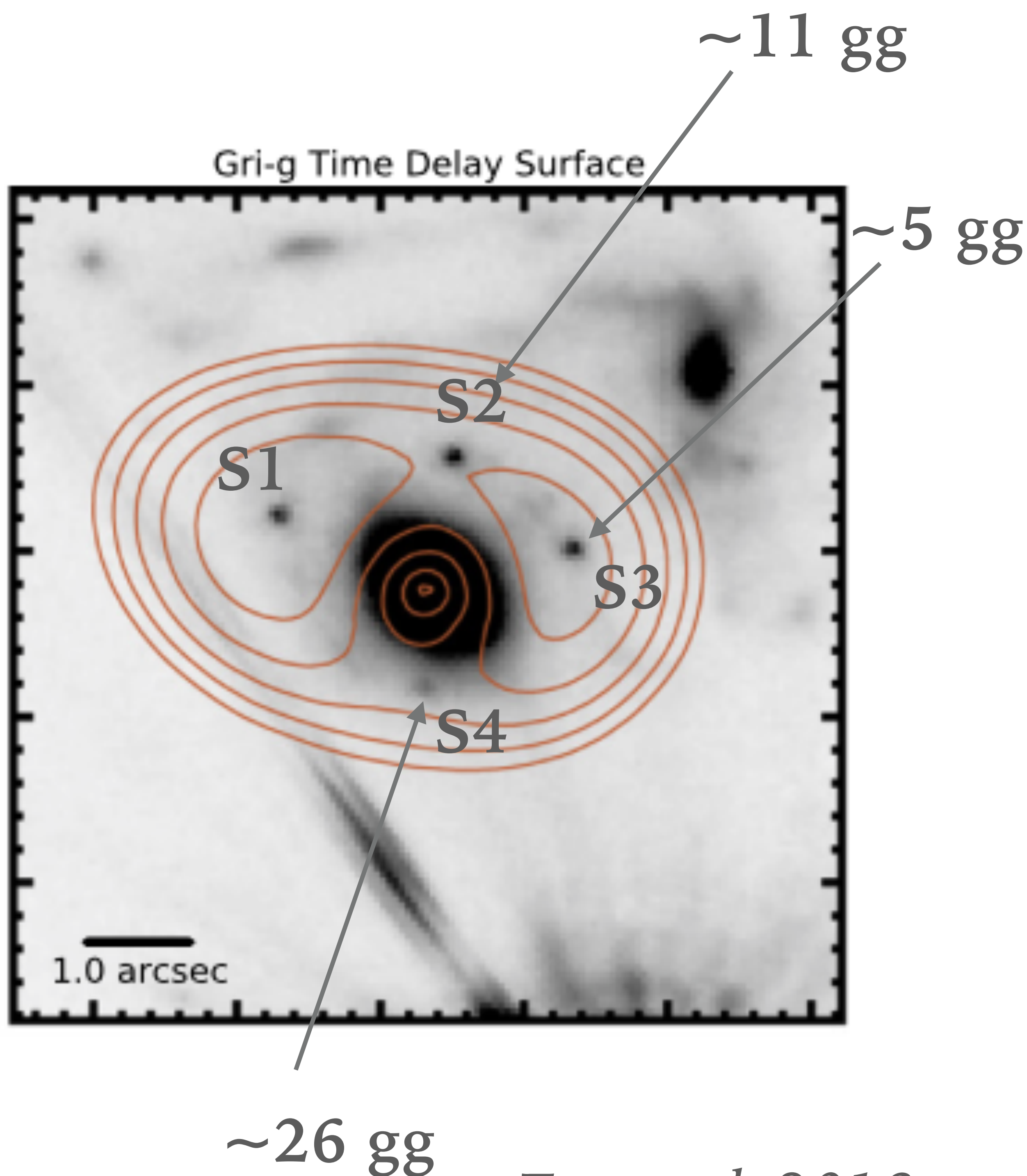

Treu et al. 2016

SN REFSDAL IN MACS 1149

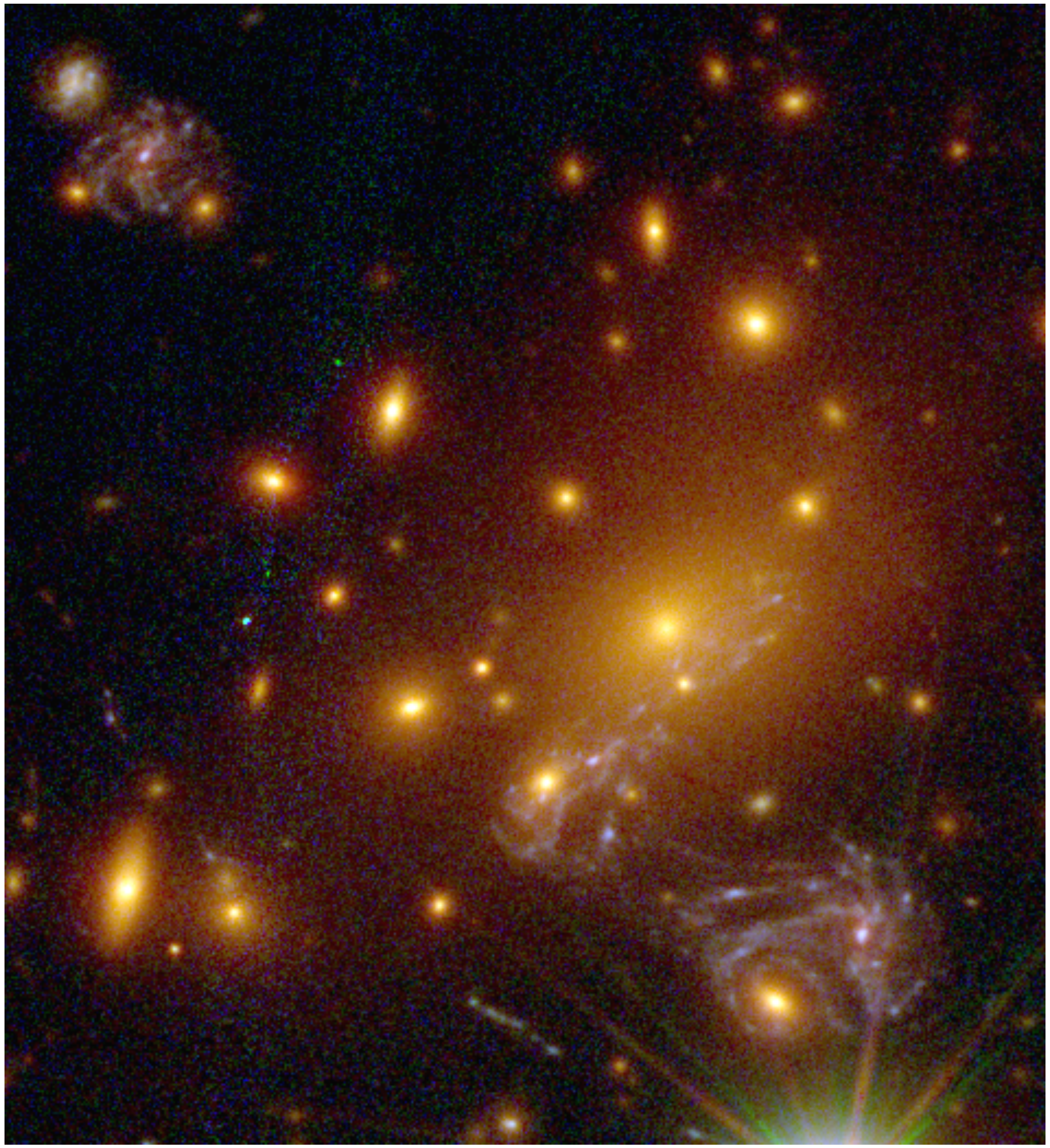

SN REFSDAL IN MACS 1149

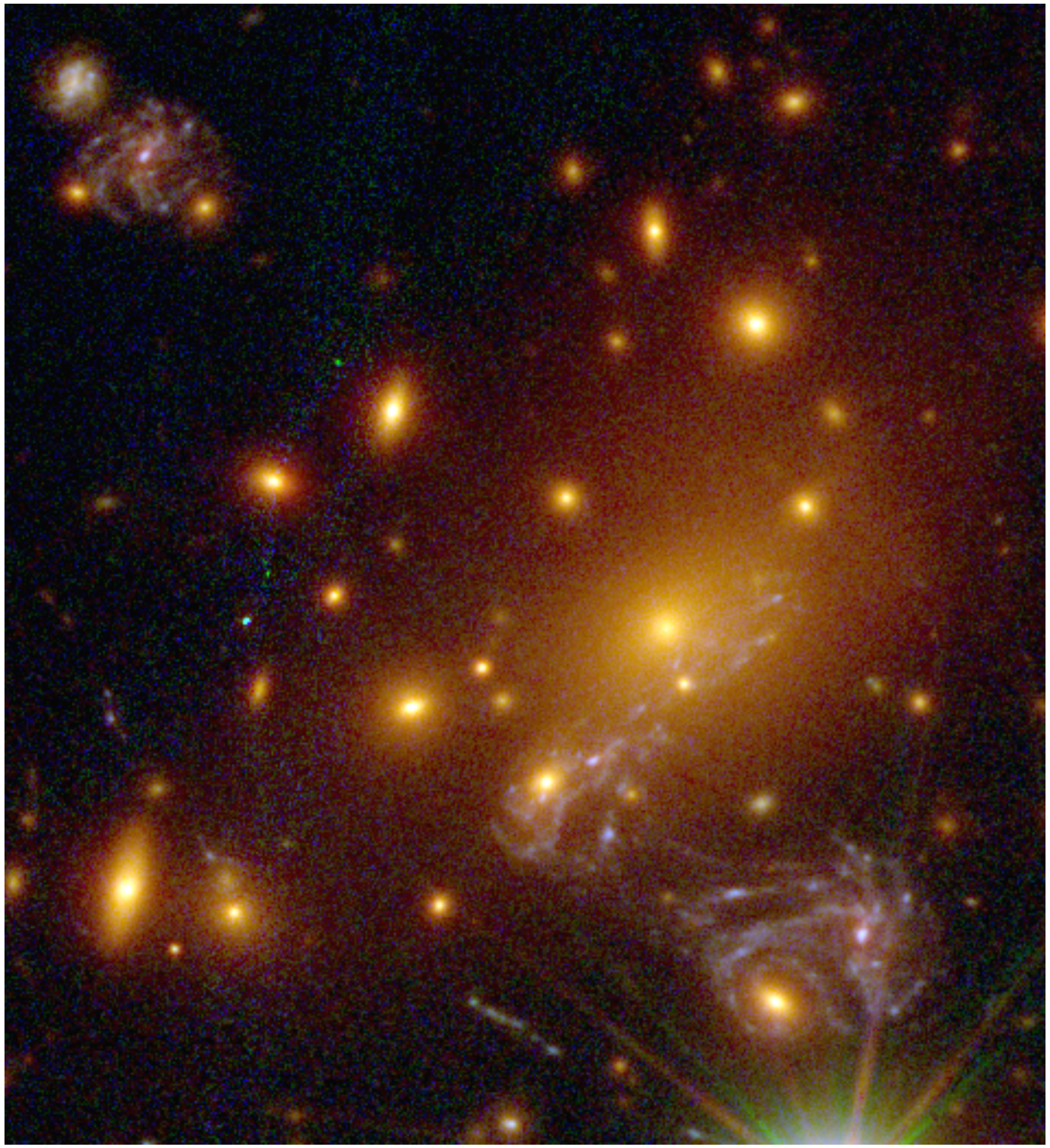

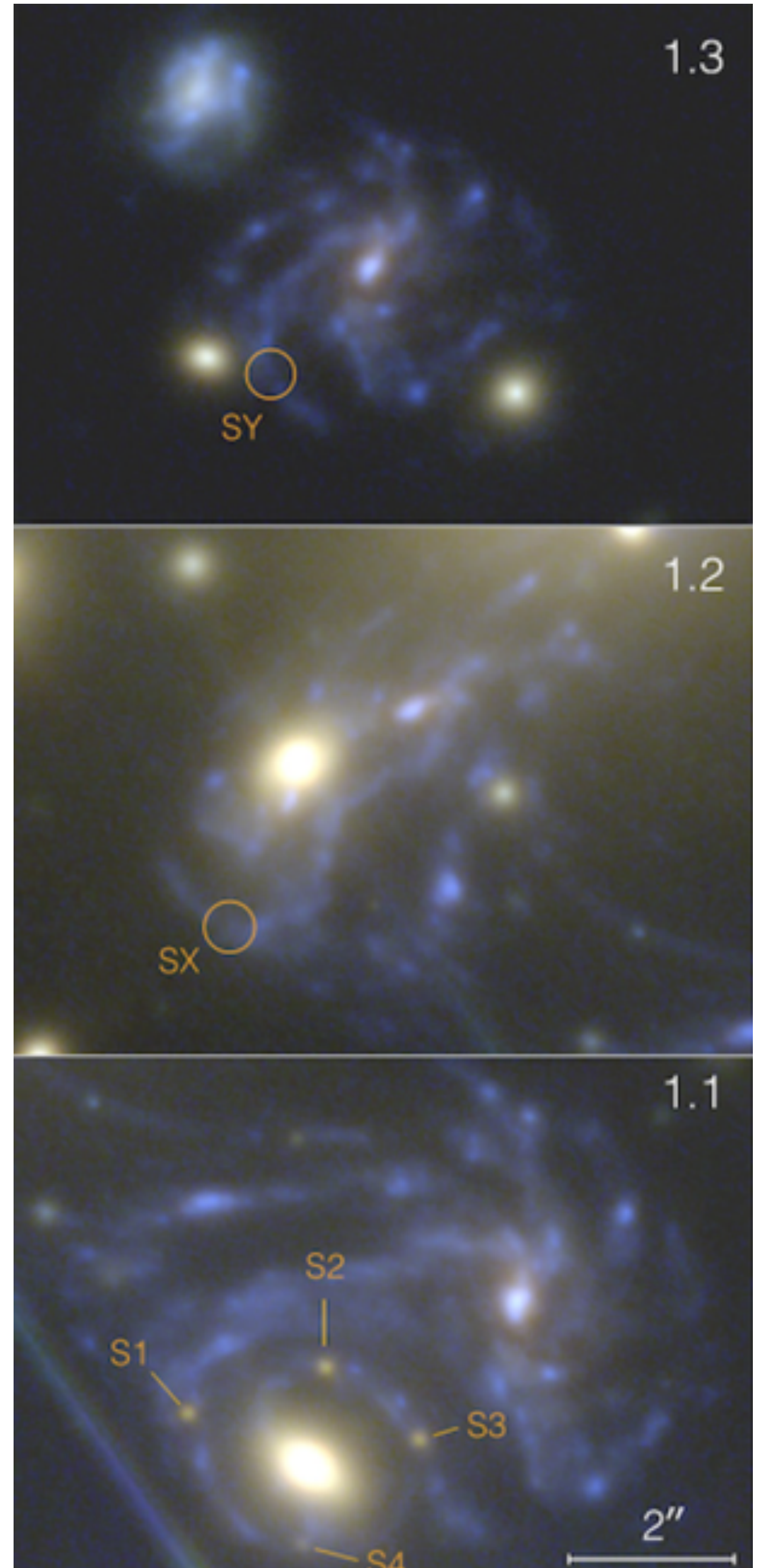

?

SN REFSDAL IN MACS 1149

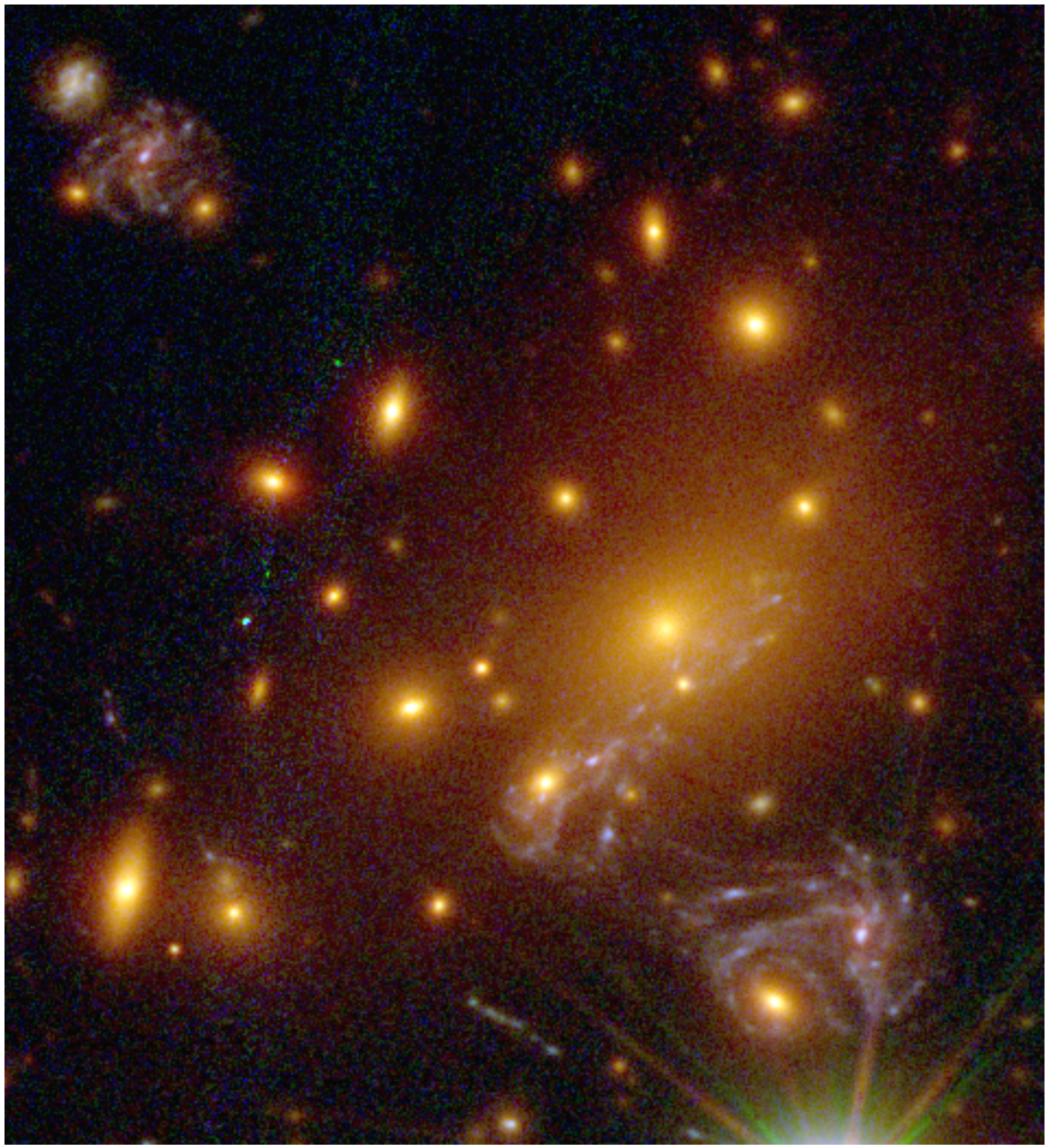

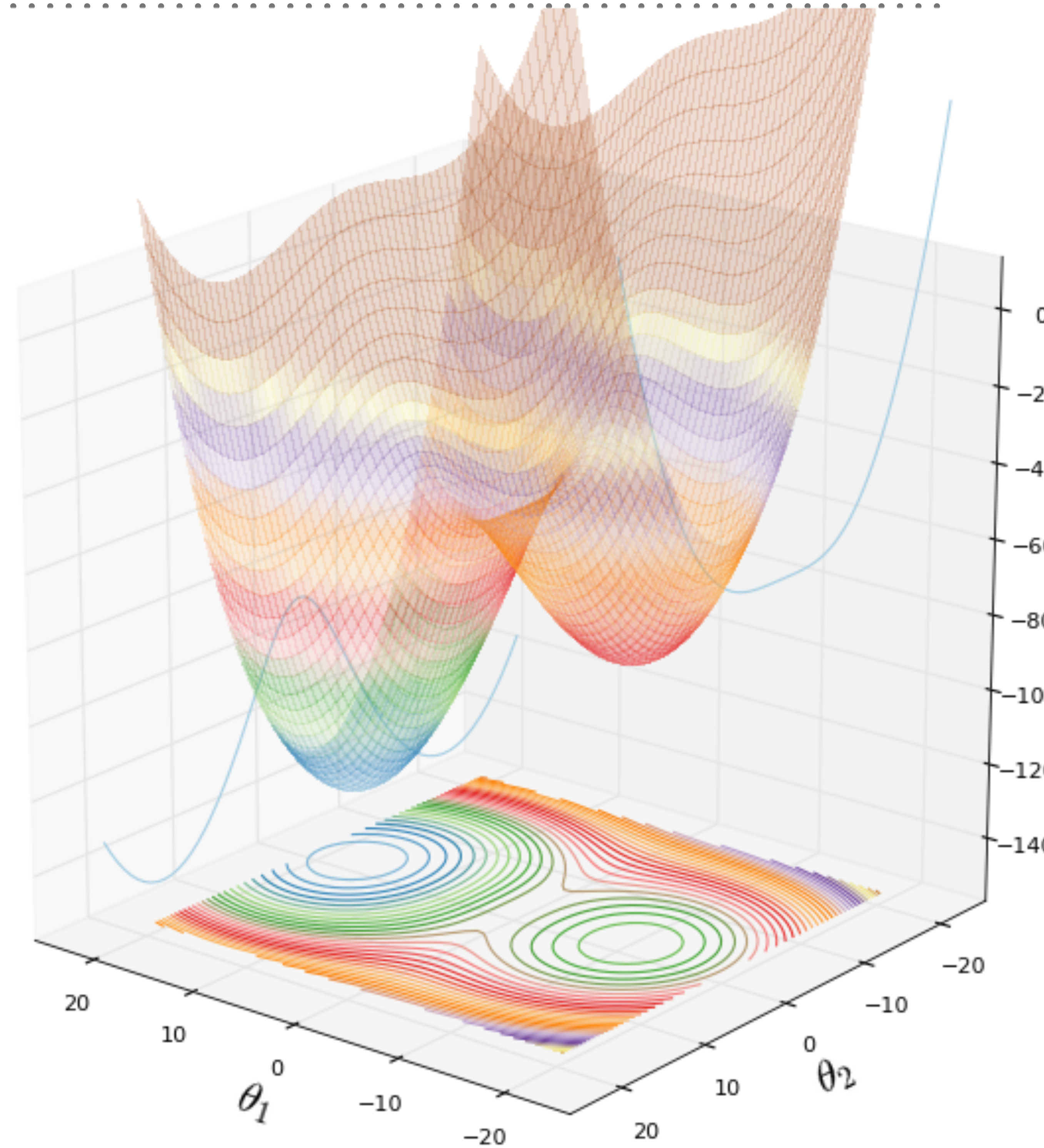

SN REFSDAL IN MACS 1149

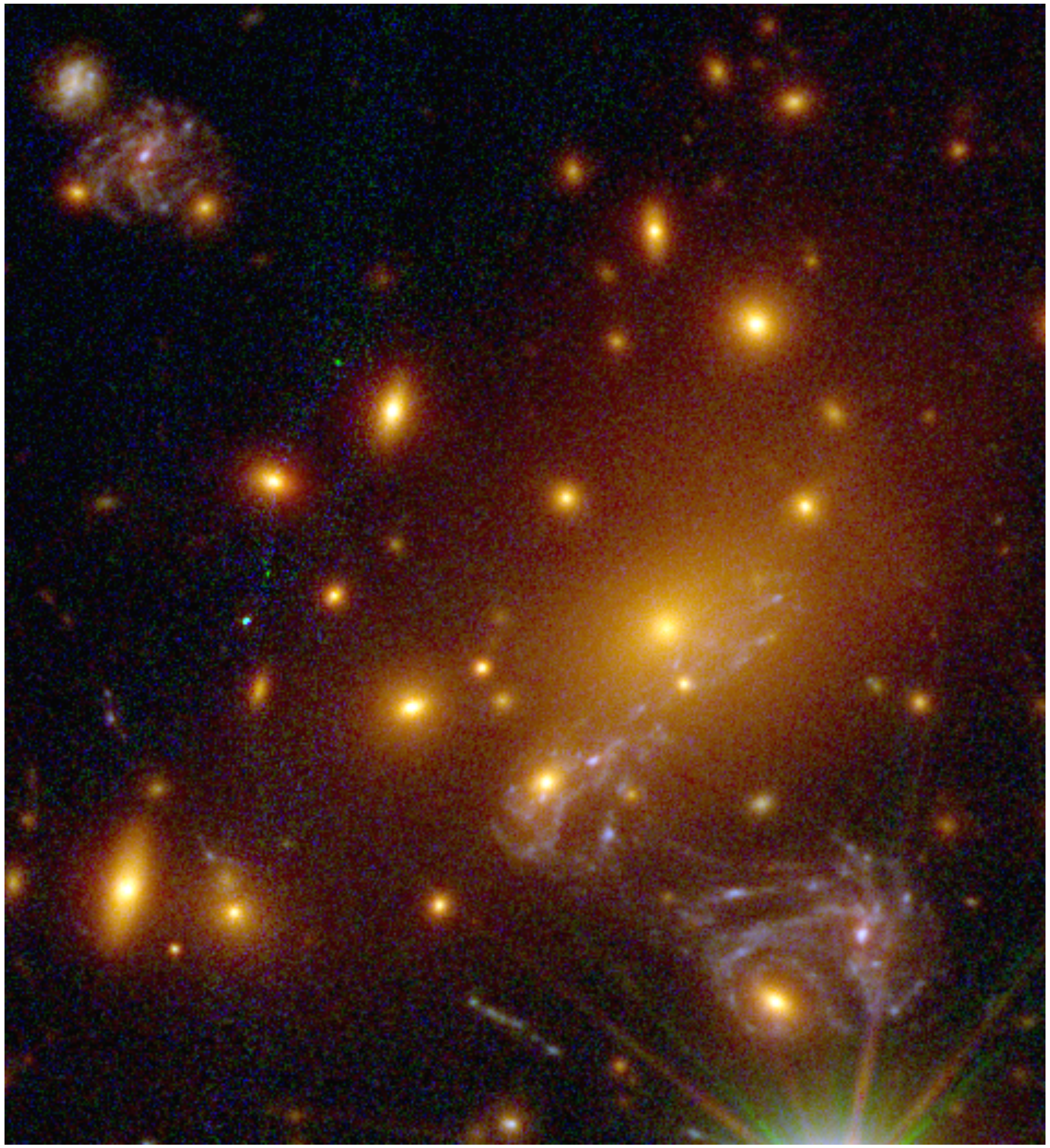

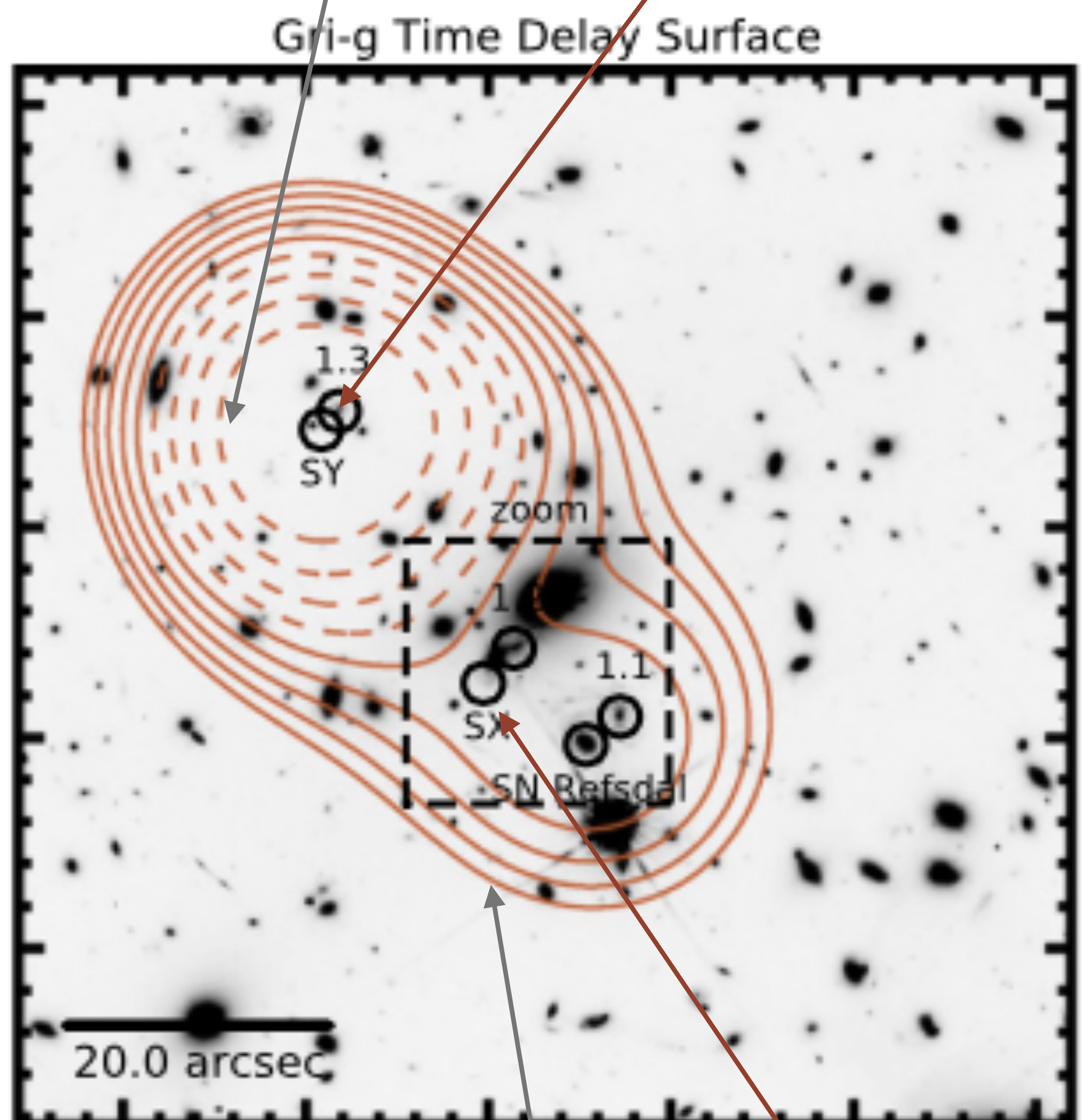

SN REFSDAL IN MACS 1149

16/12/2016…

Time delay

(SX- S1) 345+-10gg

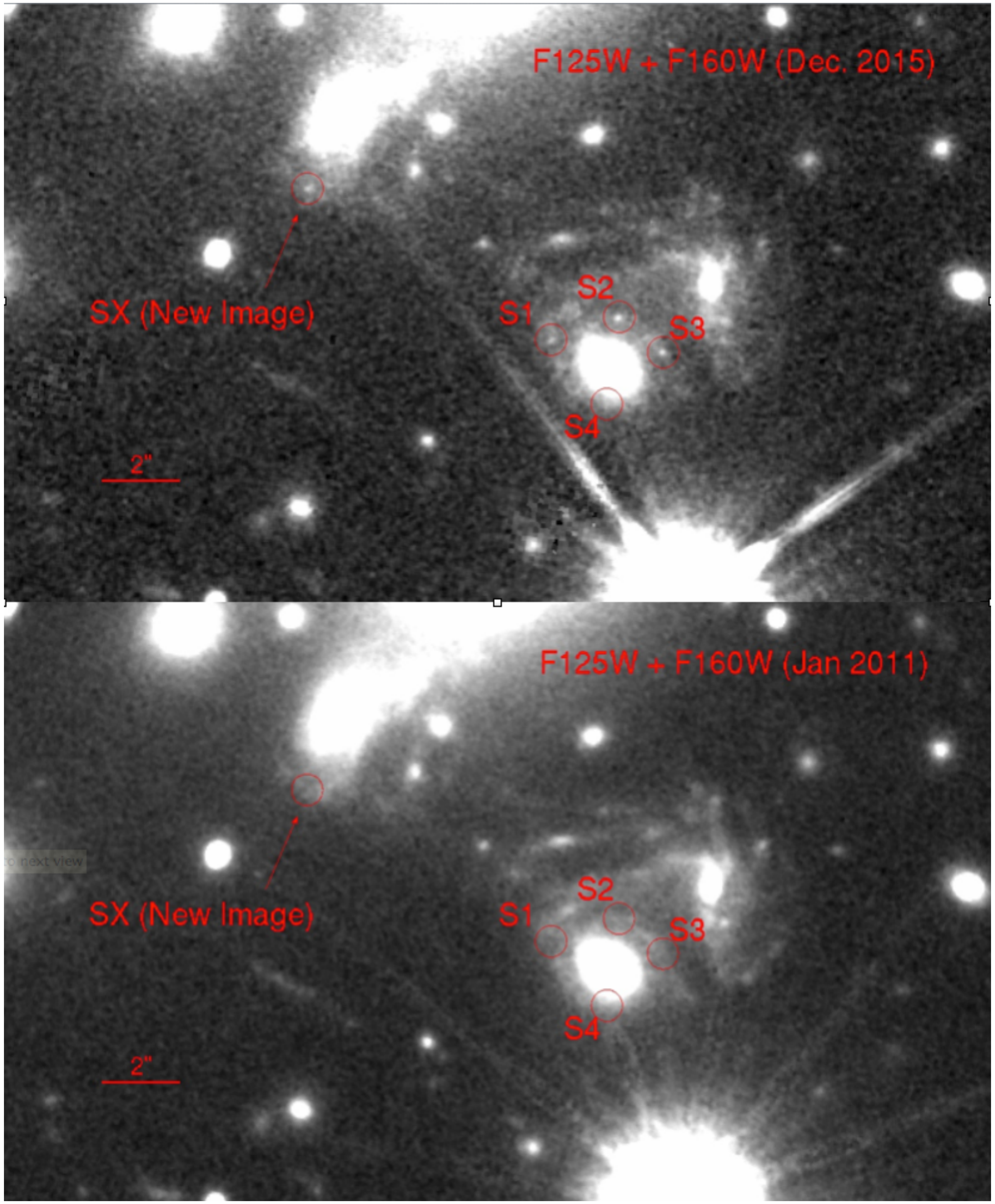

H0 (AND OTHER COSMOLOGICAL PARAMETERS) FROM REFSDAL

MACSJ119 also contains 10 families of multiple images with $1.2 < z < 3.7$

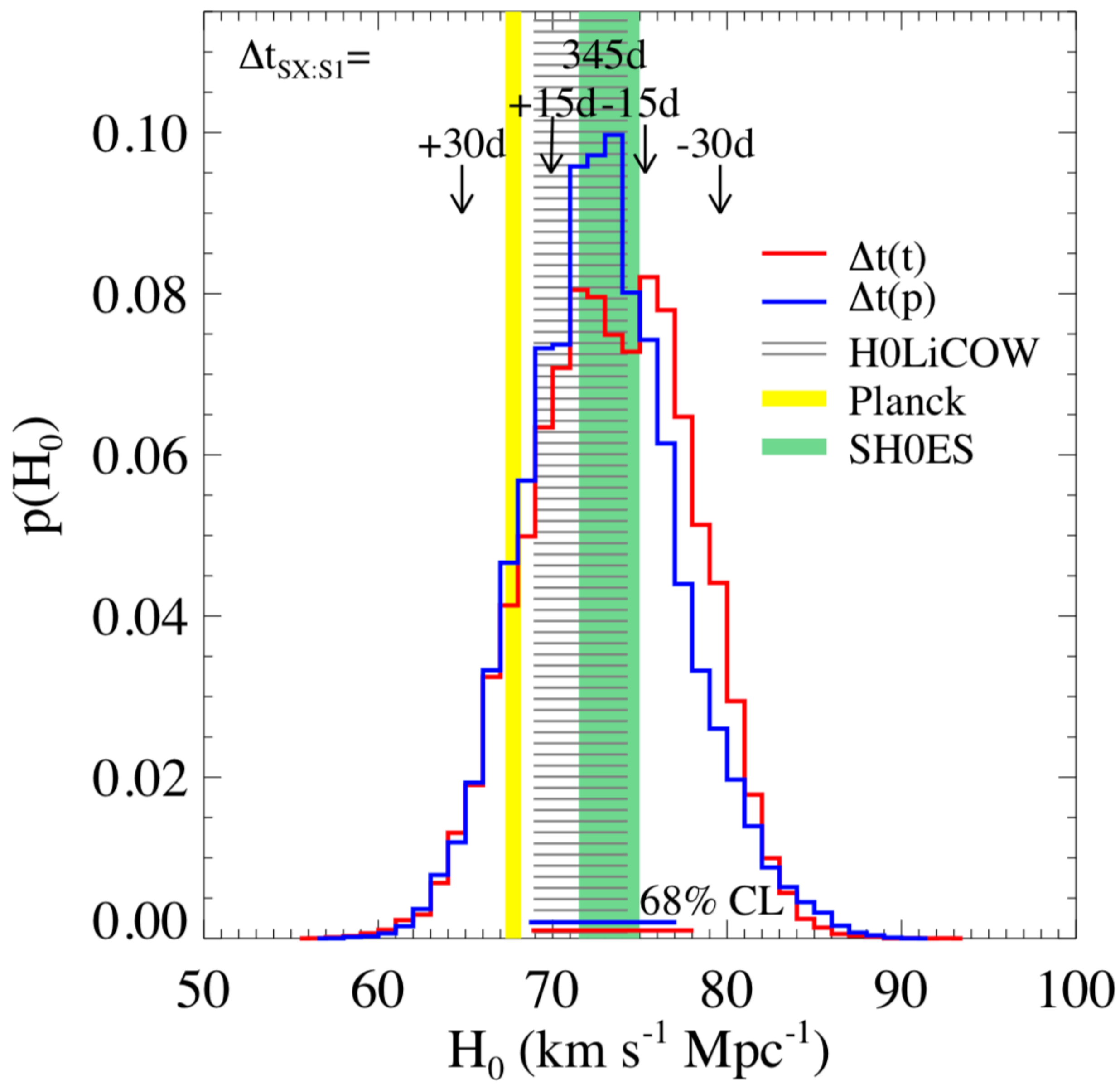

Grillo et al. (2018)

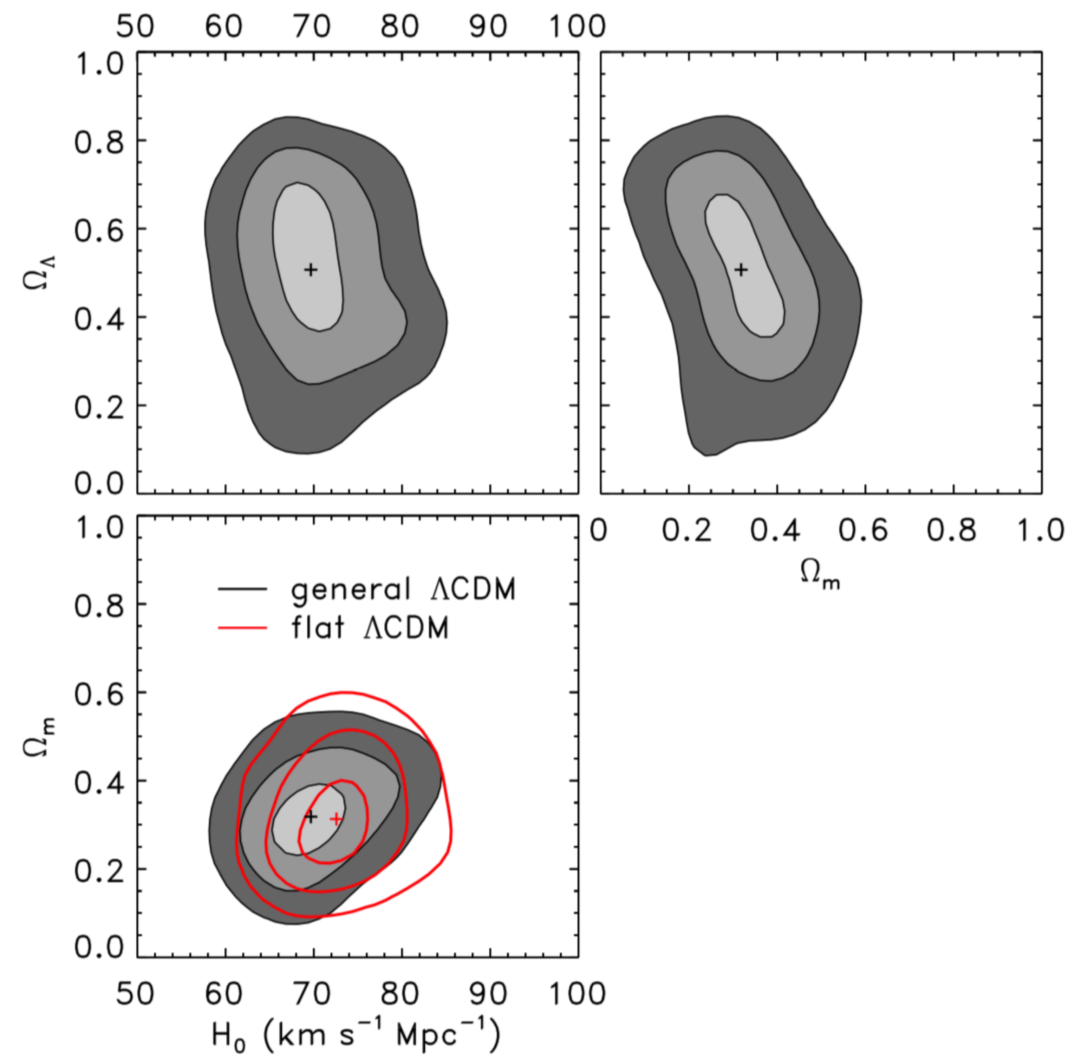

fitting in a flat LCDM

OTHER MULTIPLY IMAGED SOURCES IN MACS1149

MACSJ119 also contains 10 families of multiple images with $1.2 < z < 3.7$

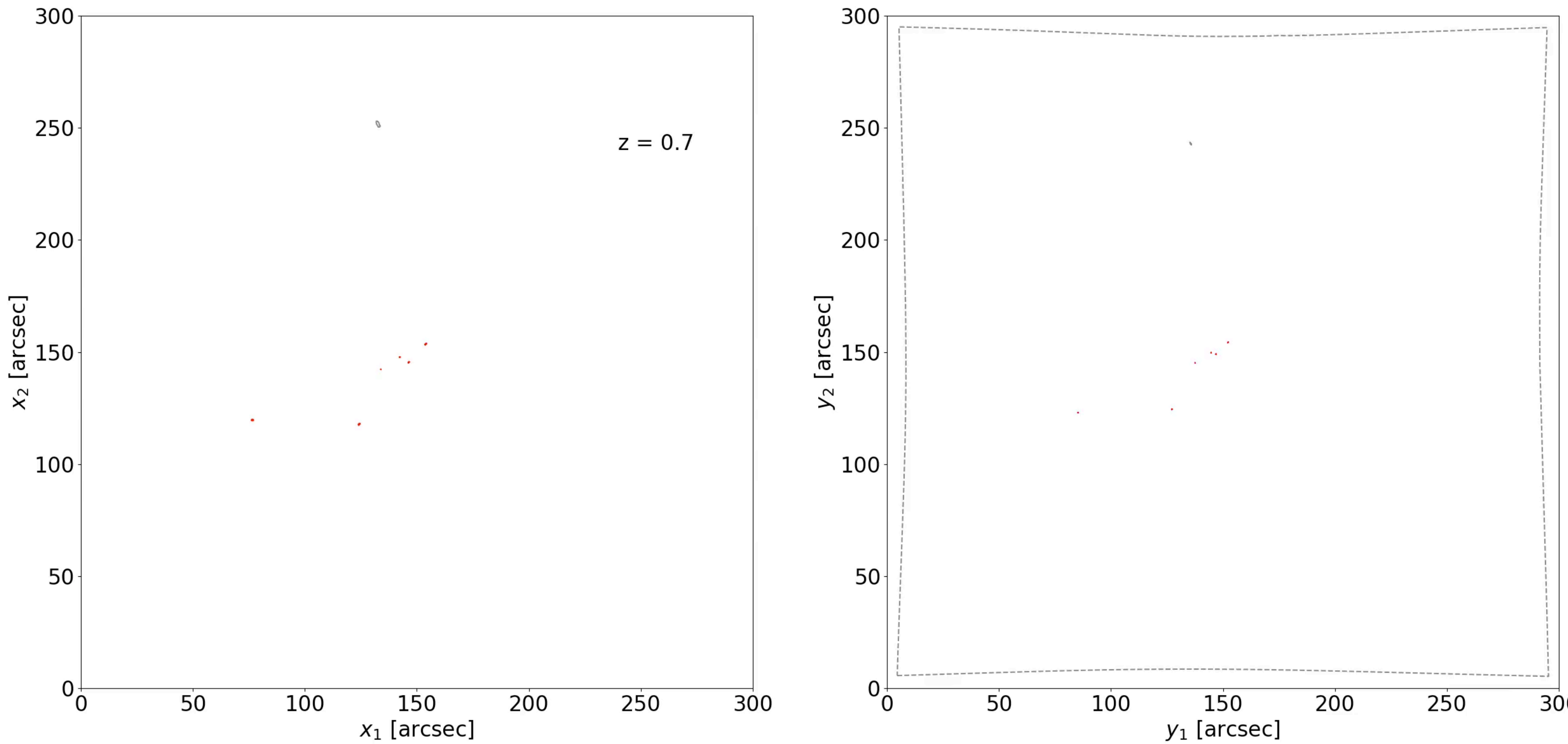

OTHER MULTIPLY IMAGED SOURCES IN MACS1149

MACSJ119 also contains 10 families of multiple images with $1.2 < z < 3.7$

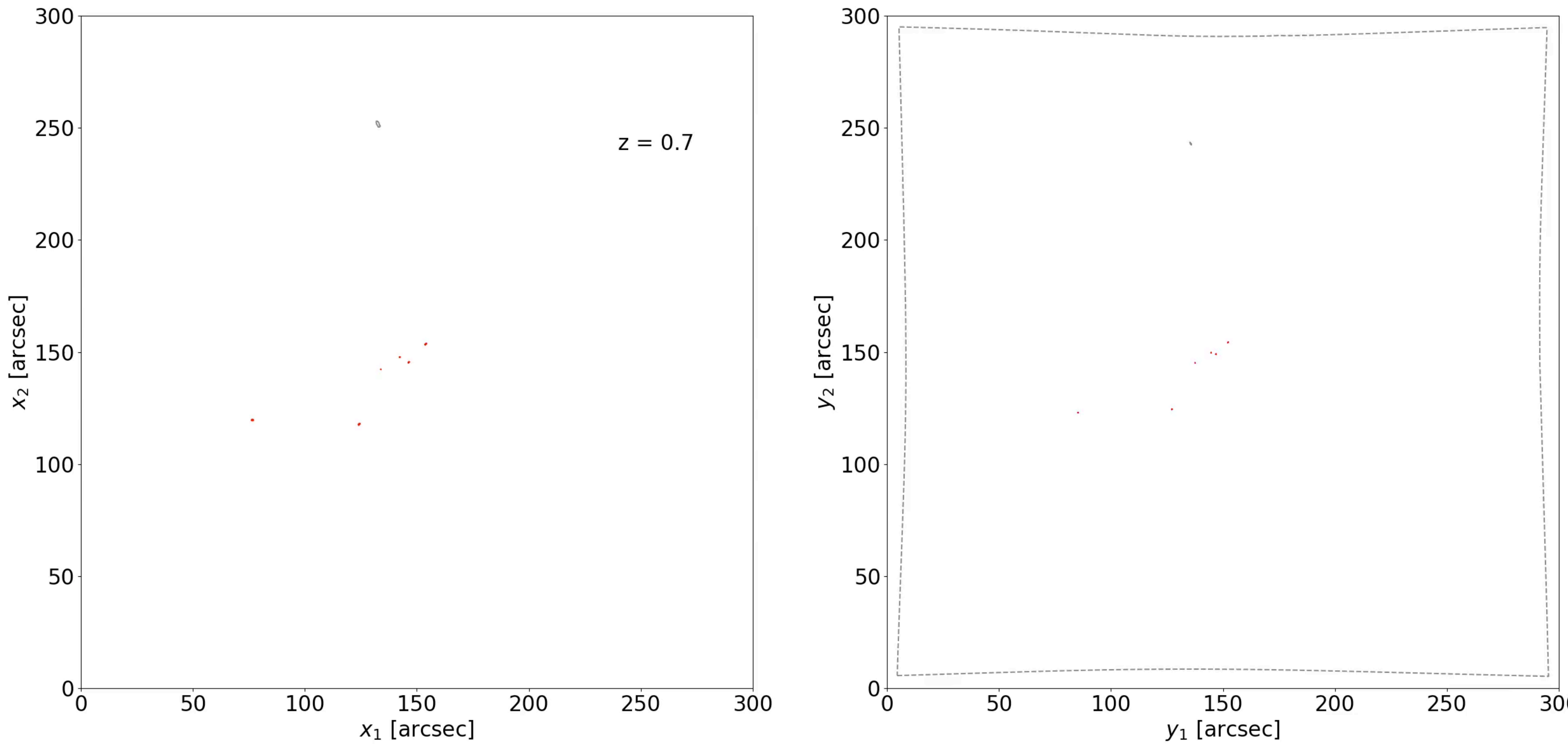

A370: first gravitational arc ever discovered in a cluster (Soucail et al. 1987; Lynds & Petrosian, 1986)

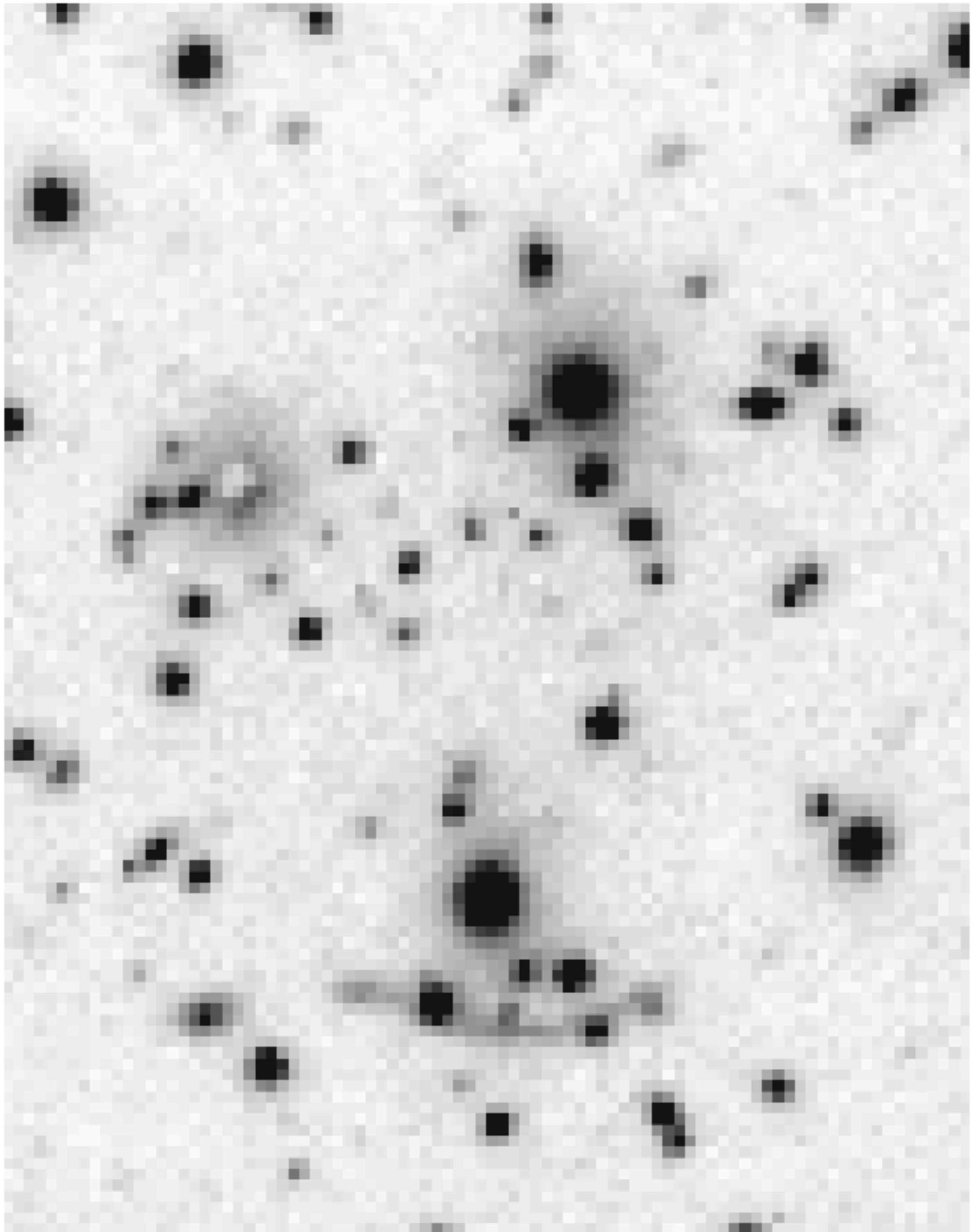

CFHT (R-band, 1985)

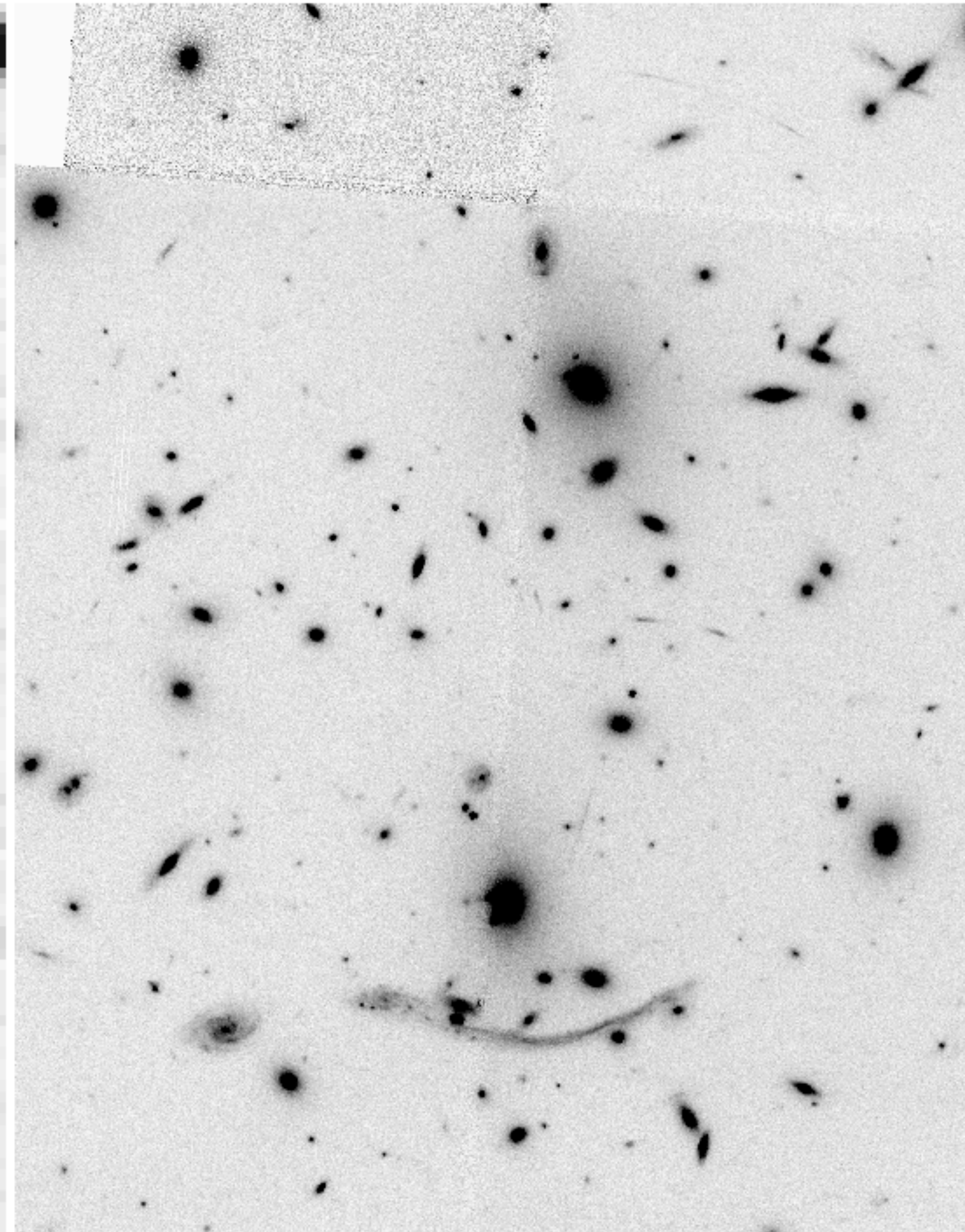

HST WFPC2 (F675W, 1995)

SL BY CLUSTERS: THE BEST DATASETS

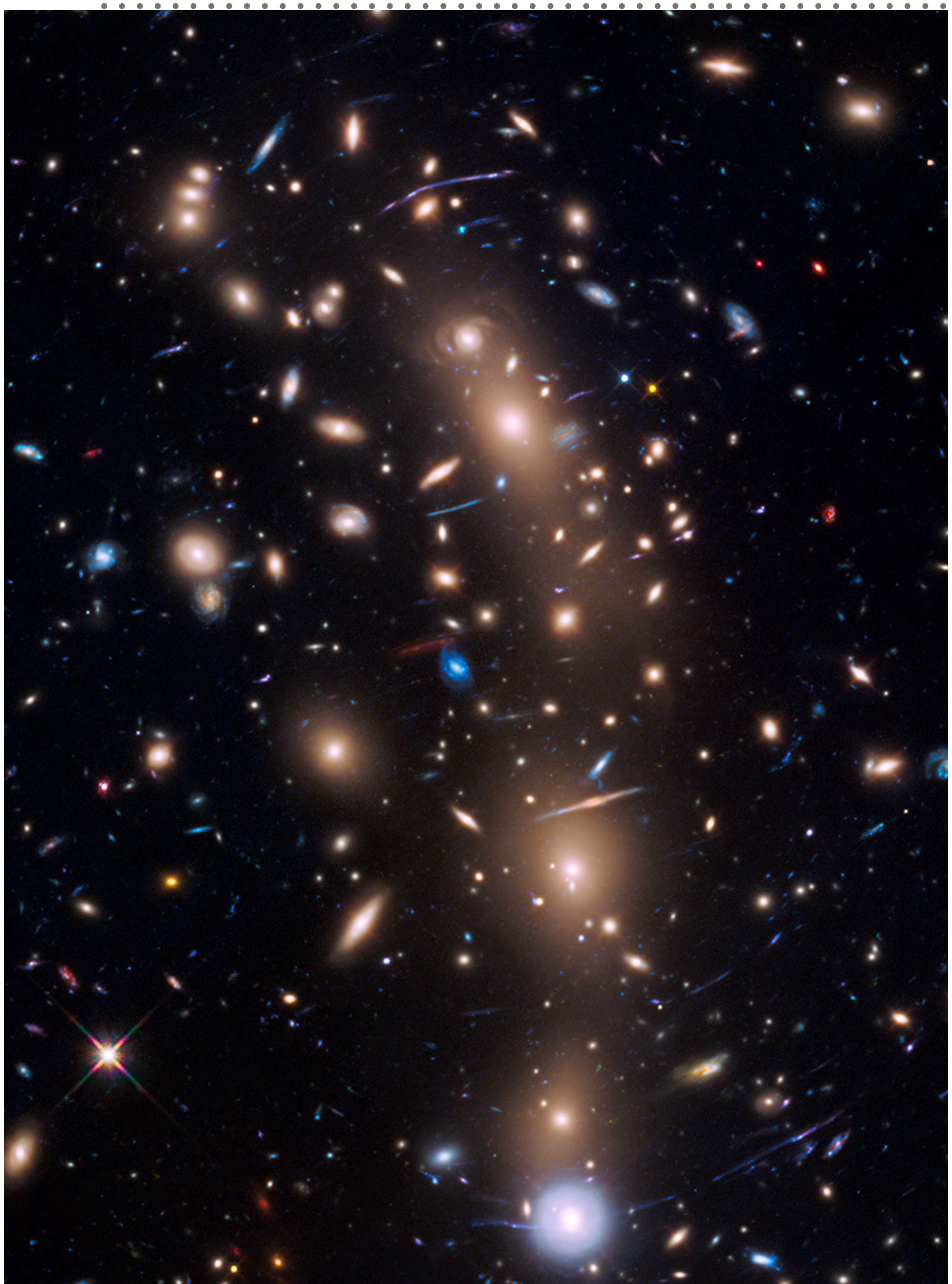

- Two SL focused Hubble MCT programs in the last 6 years
- CLASH (PI Postman, 25 clusters, 525 orbits, 16 bands)
- **Frontier-Fields (PI Lotz, 6 clusters, 840 orbits, 7 bands)**
- deep, high-resolution imaging from UV to NIR
- $m_{int}=m_{obs}+2.5\log10(\mu)$

ACS: (70 orbits per position)			WFC3/IR: (70 orbits per position)		
Filter	Orbits	AB_mag	Filter	Orbits	AB_mag
F435W	18	28.8	F105W	24	28.9
F606W	10	28.8	F125W	12	28.6
F814W	42	29.1	F140W	10	28.6
			F160W	24	28.7

SL BY CLUSTERS: THE BEST DATASETS

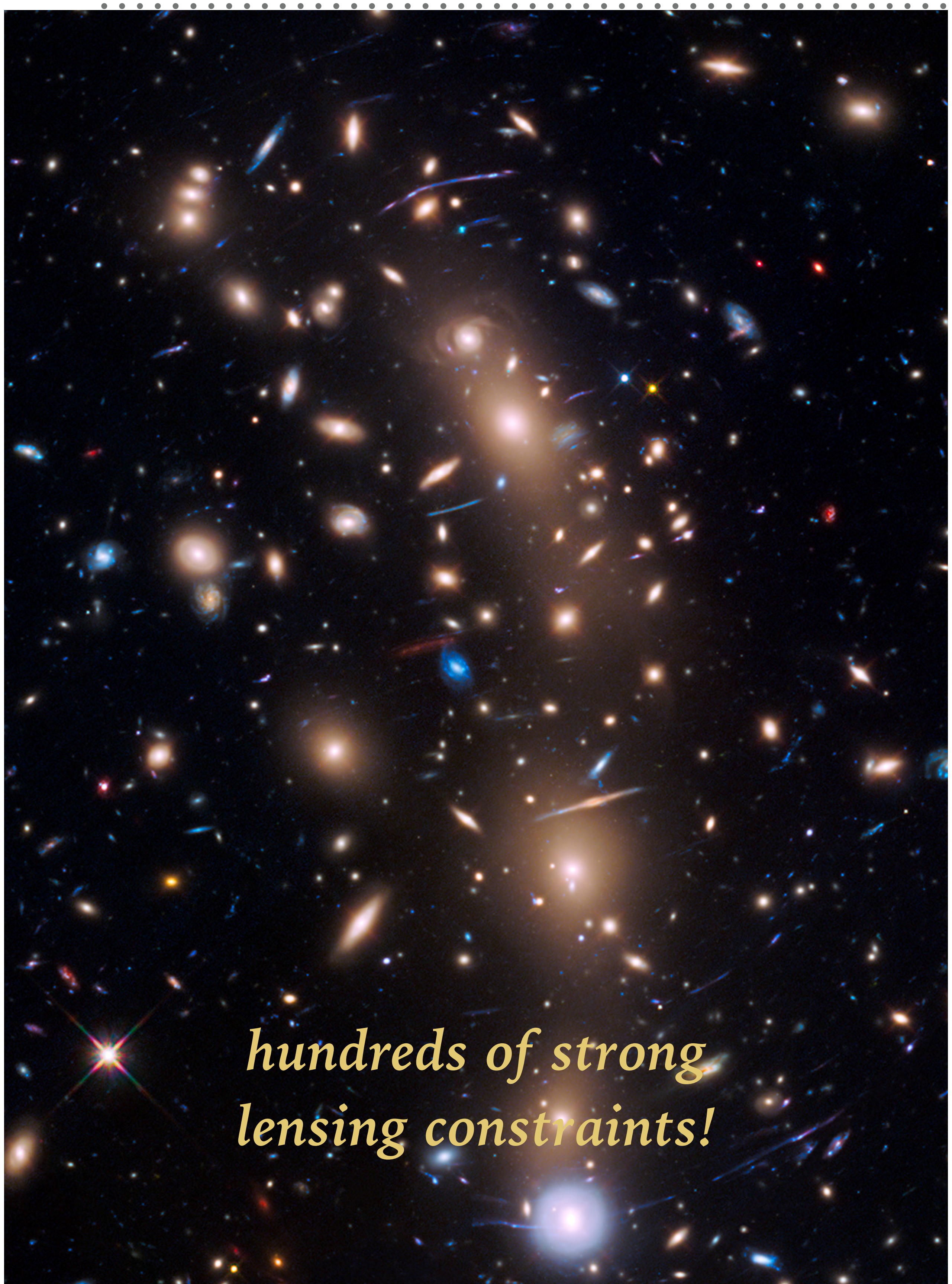

- Two SL focused Hubble MCT programs in the last 6 years
- CLASH (PI Postman, 25 clusters, 525 orbits, 16 bands)
- **Frontier-Fields (PI Lotz, 6 clusters, 840 orbits, 7 bands)**
- deep, high-resolution imaging from UV to NIR
- $m_{int}=m_{obs}+2.5\log10(\mu)$

ACS: (70 orbits per position)			WFC3/IR: (70 orbits per position)		
Filter	Orbits	AB_mag	Filter	Orbits	AB_mag
F435W	18	28.8	F105W	24	28.9
F606W	10	28.8	F125W	12	28.6
F814W	42	29.1	F140W	10	28.6
			F160W	24	28.7

A370 after the FF program

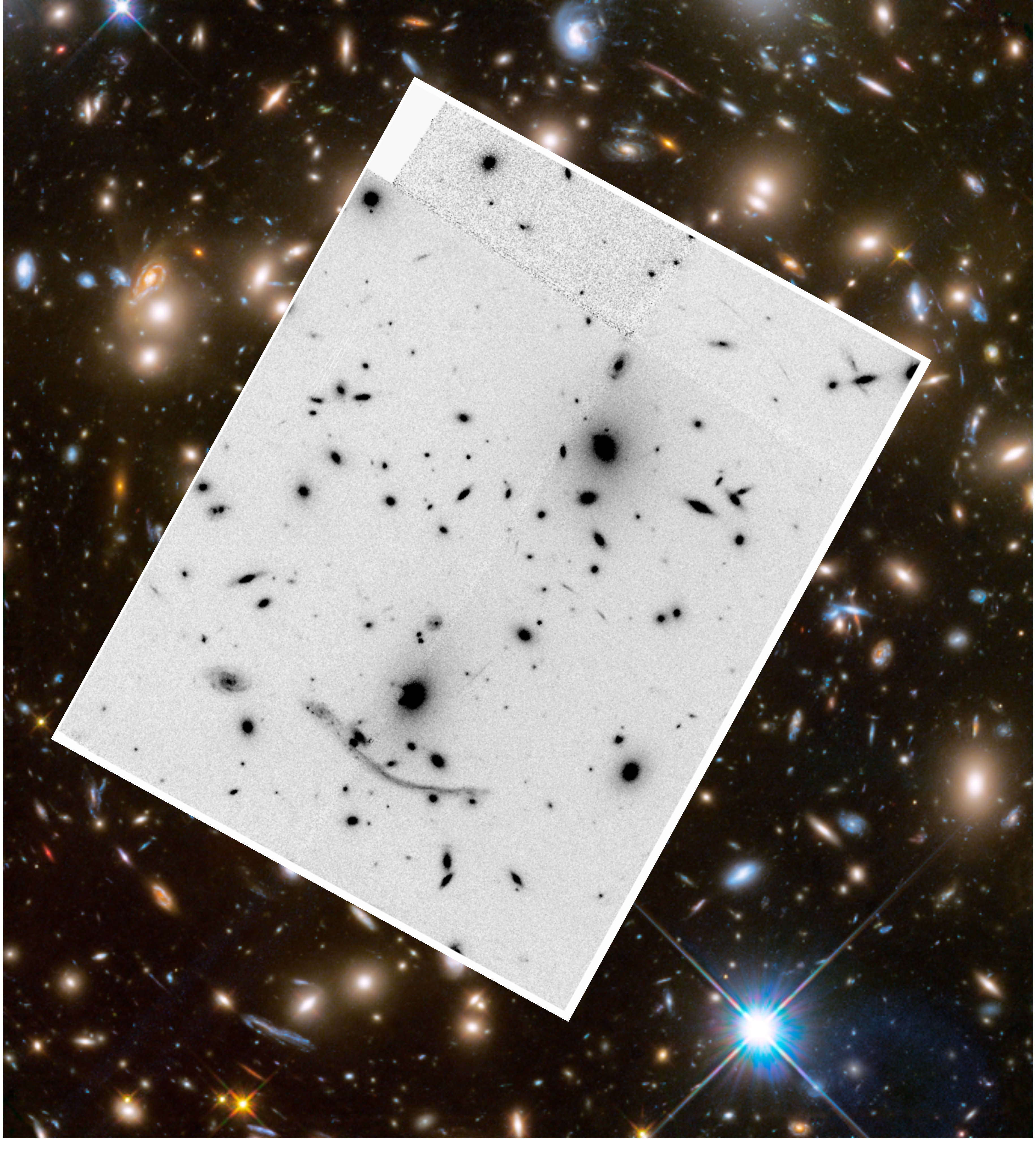

A370 after the FF program

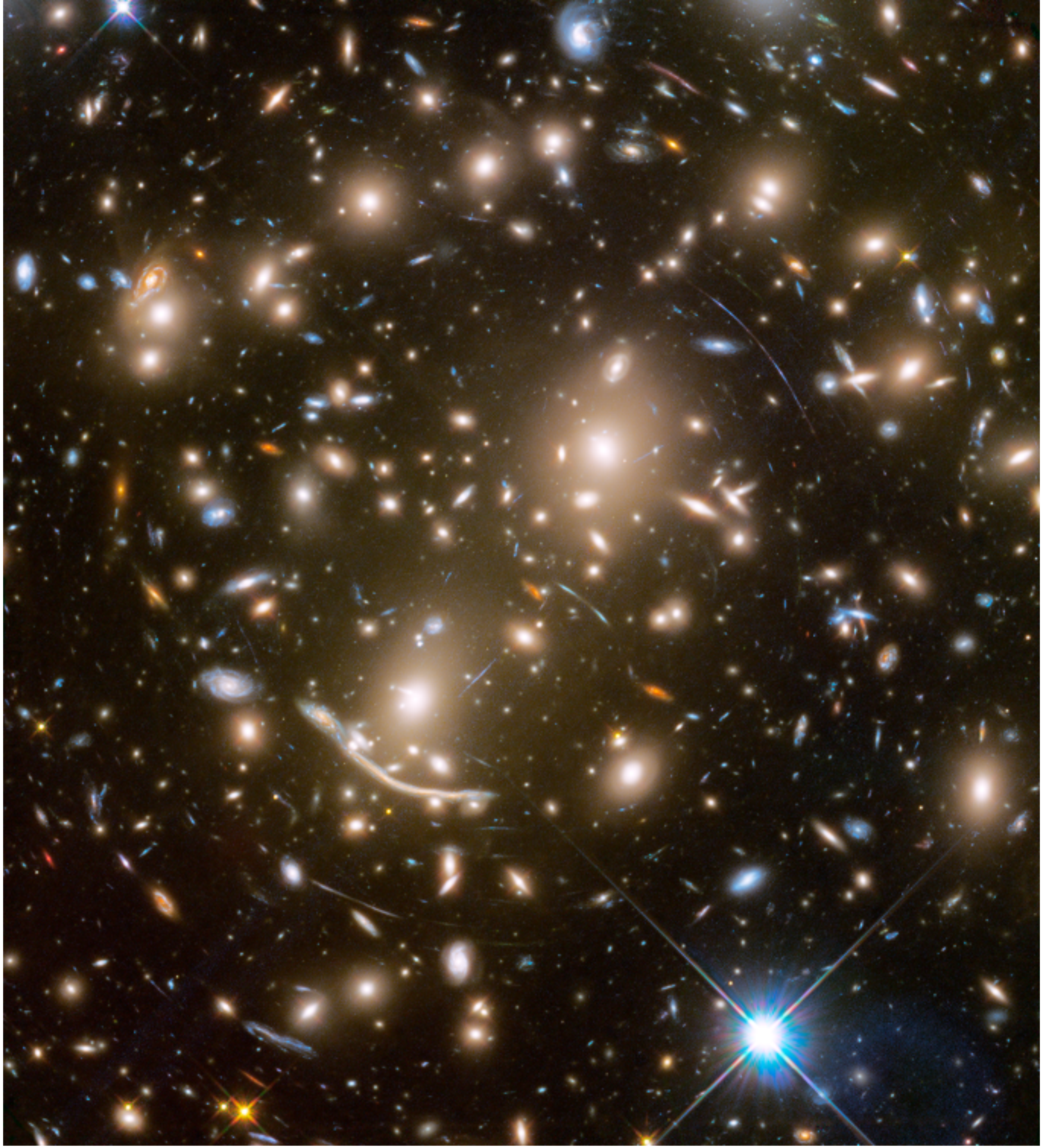

MACSJ0416 **1. Before HFF ...**

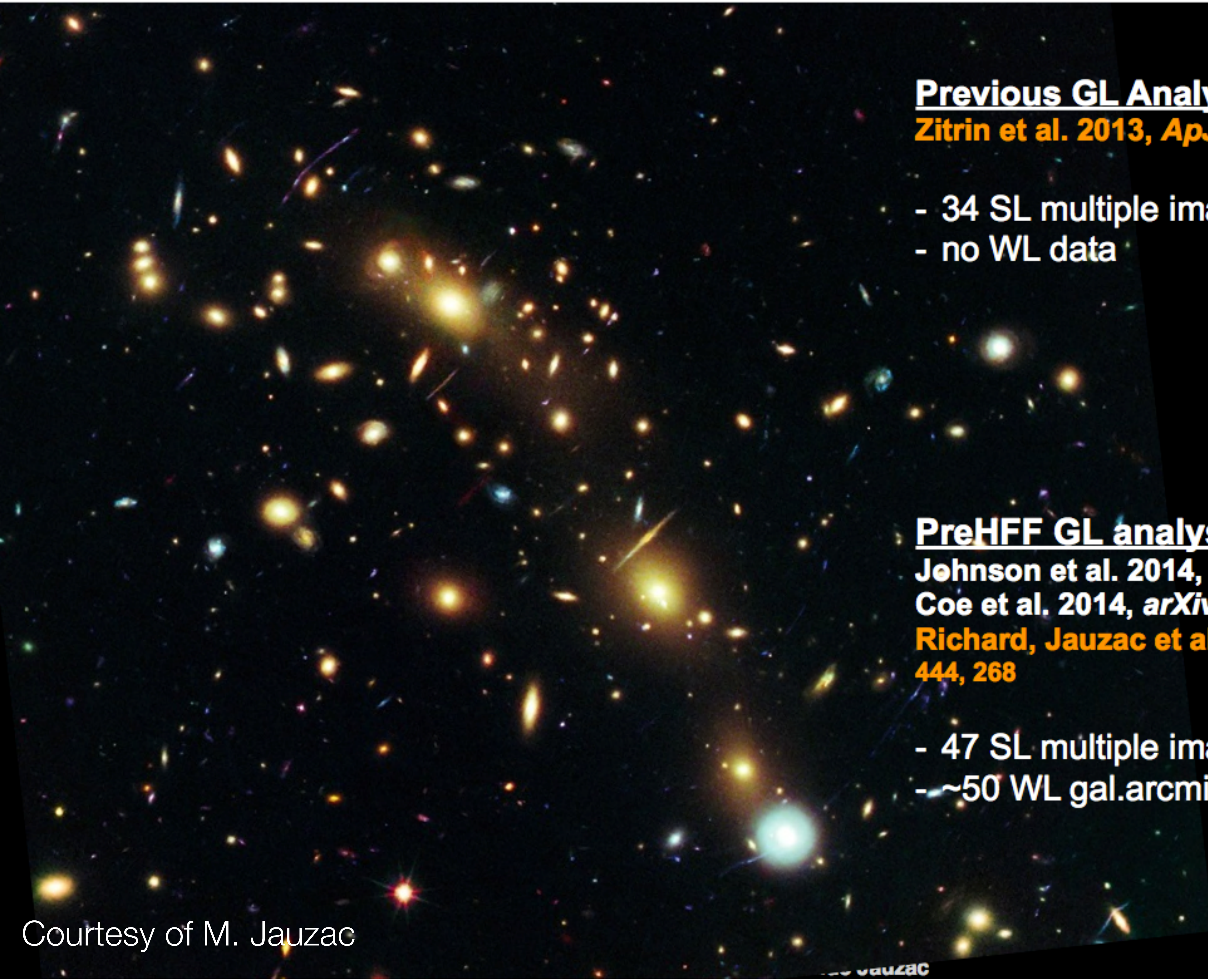

<u>Previous GL Analysis :</u>
Zitrin et al. 2013, *ApJ, 762, 30*

- 34 SL multiple images
- no WL data

<u>PreHFF GL analysis :</u>
Johnson et al. 2014, *arXiv 1405.0222*
Coe et al. 2014, *arXiv 1405.0011*
Richard, Jauzac et al. 2014, MNRAS, 444, 268

- 47 SL multiple images
- ~50 WL gal.arcmin^{-2}

Courtesy of M. Jauzac

1. … After HFF !!!

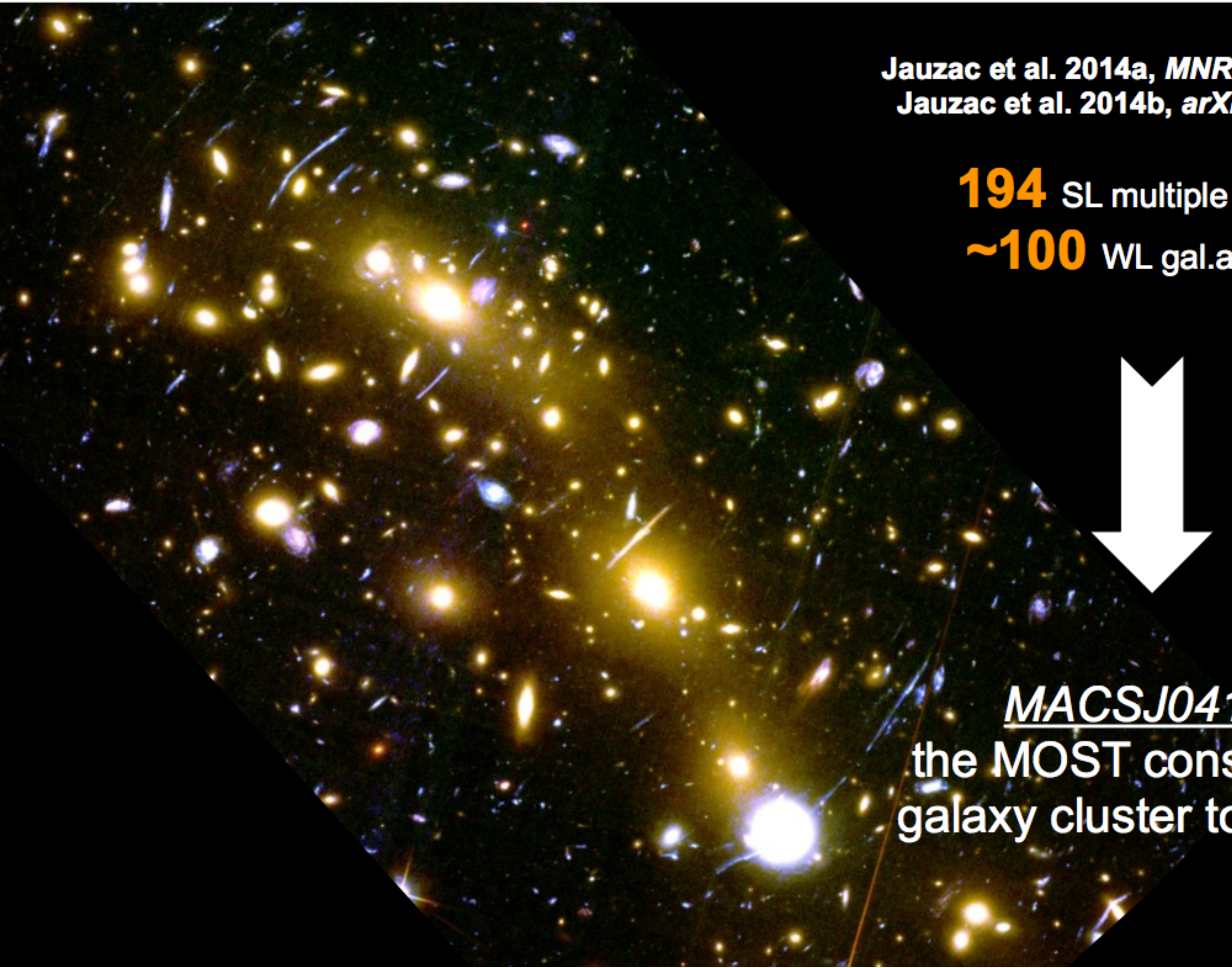

Jauzac et al. 2014a, *MNRAS, 443, 1549*
Jauzac et al. 2014b, *arXiv, 1406.3011*

194 SL multiple images
~100 WL gal.arcmin^{-2}

MACSJ0416 :
the MOST constrained galaxy cluster to date !!!

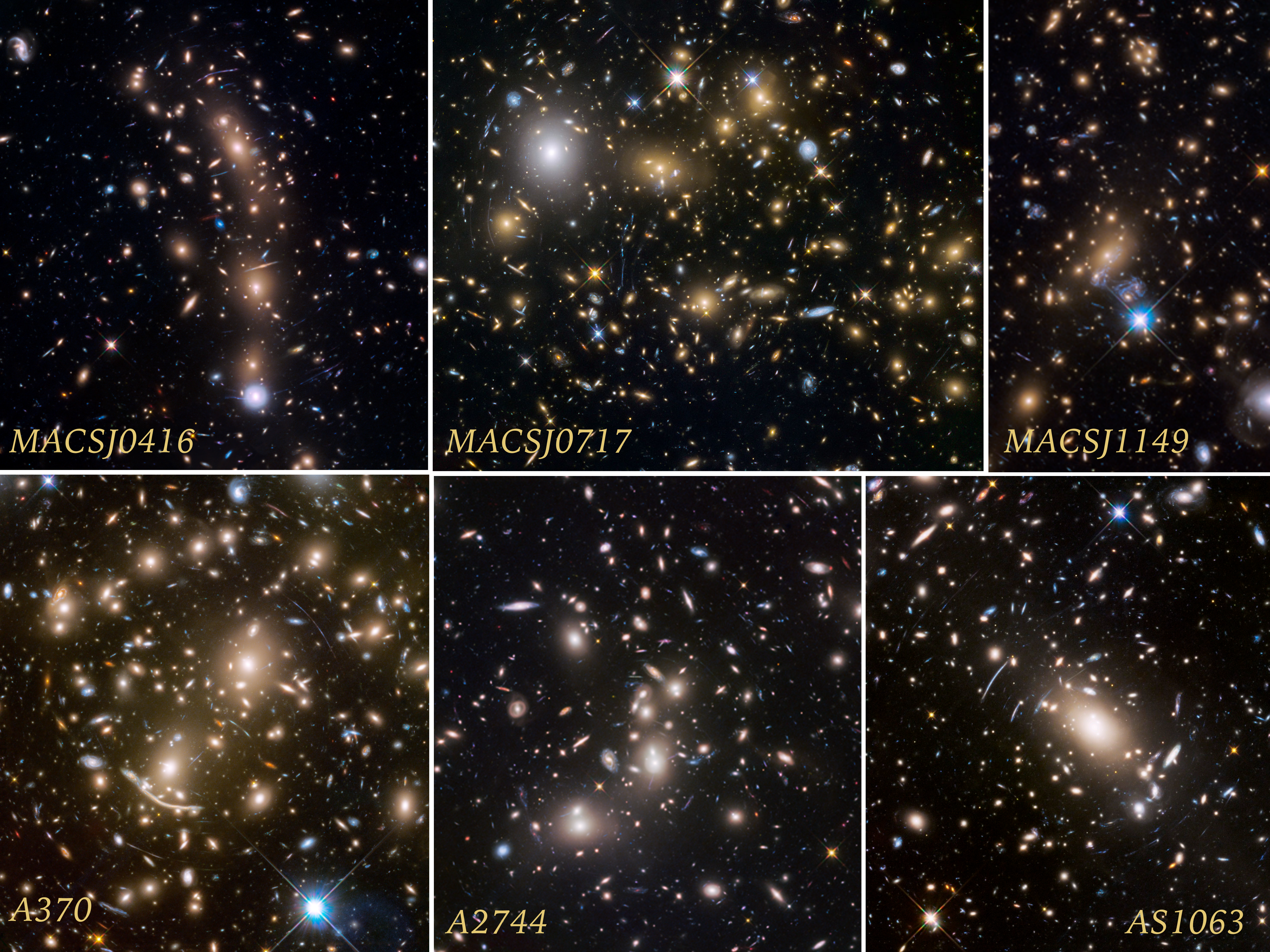
MACSJ0416
MACSJ0717
MACSJ1149
A370
A2744
AS1063

COSMIC TELESCOPES

- use the enormous magnification power of galaxy clusters to detect and characterize distant, intrinsically small and/or faint sources [re-ionization, build-up of galaxies, proto-globular clusters]

COSMIC TELESCOPES

- use the enormous magnification power of galaxy clusters to detect and characterize distant, intrinsically small and/or faint sources [re-ionization, build-up of galaxies, proto-globular clusters]

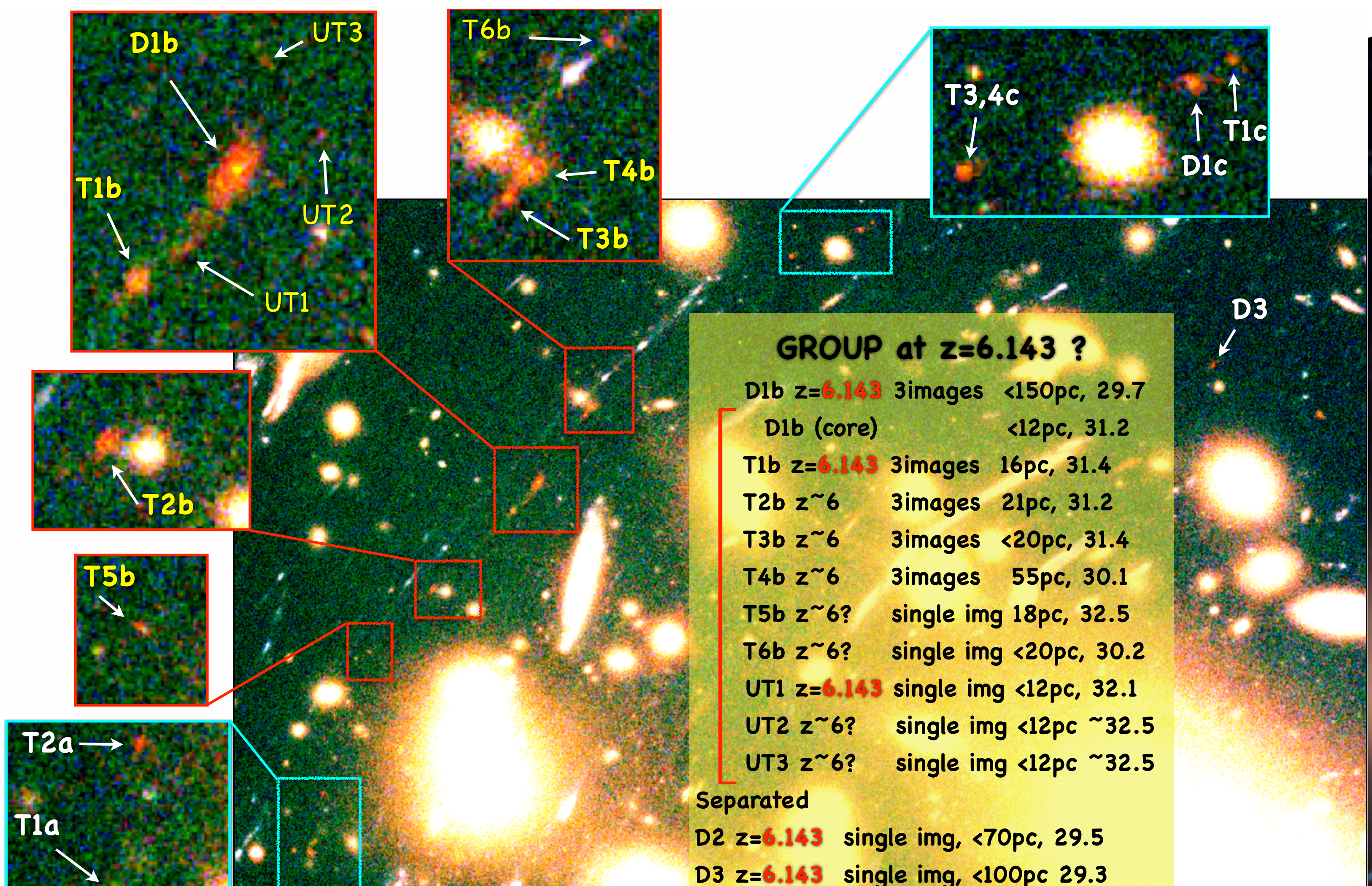

Multiple images of D1, T1, T2, T3, T4 have been identified

The zphot~6 of T2,T3,T4 are corroborated by the multiple images (low-z solutions are excluded).

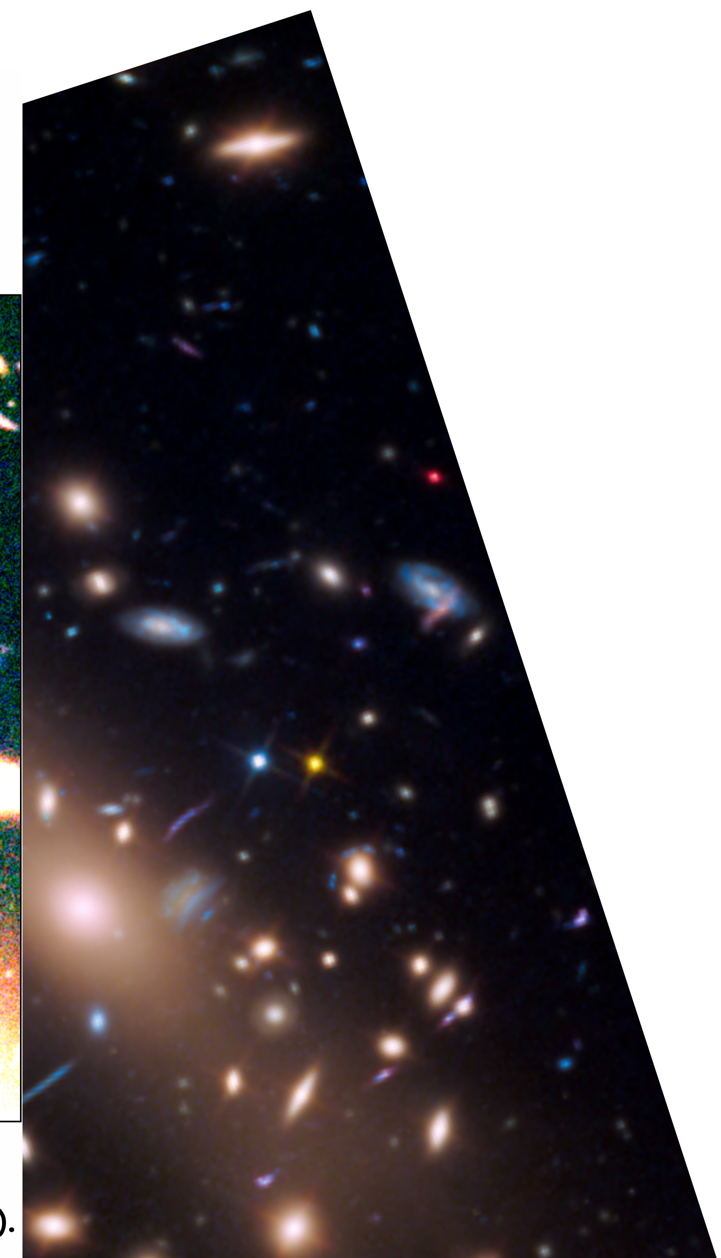

COSMIC TELESCOPES

- use the enormous magnification power of galaxy clusters to detect and characterize distant, intrinsically small and/or faint sources [re-ionization, build-up of galaxies, proto-globular clusters]

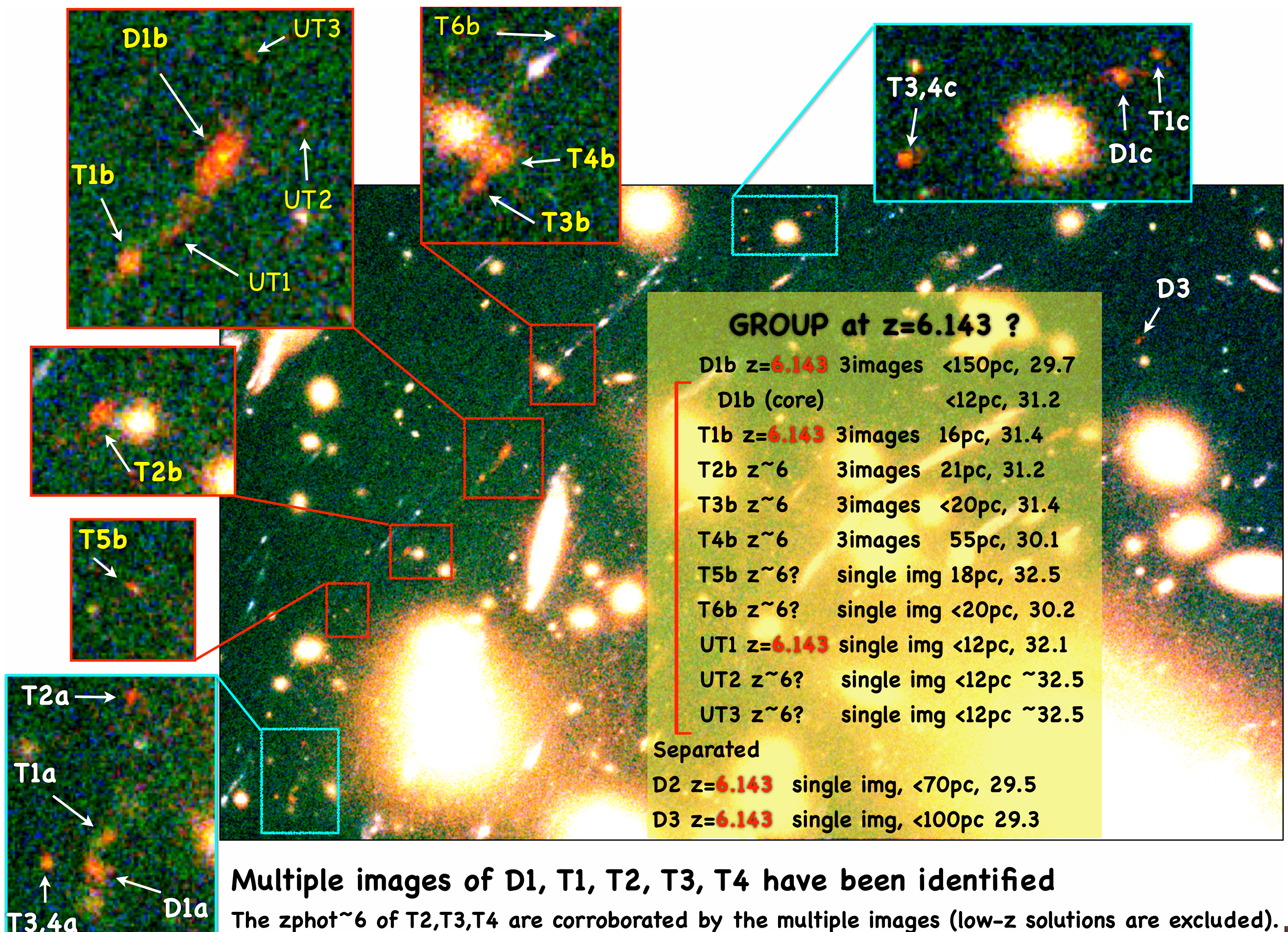

Multiple images of D1, T1, T2, T3, T4 have been identified

The zphot~6 of T2,T3,T4 are corroborated by the multiple images (low-z solutions are excluded).

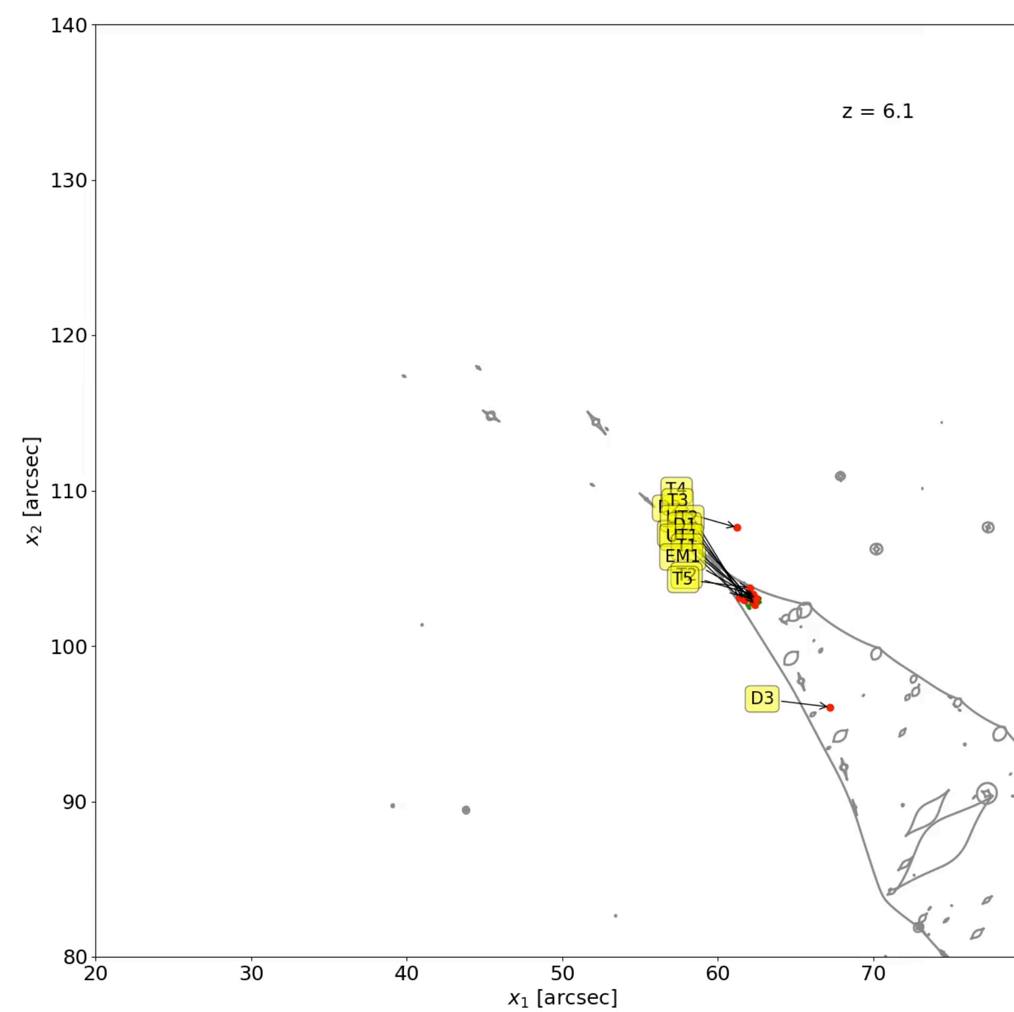

COSMIC REIONIZATION

Robertson et al. 2010

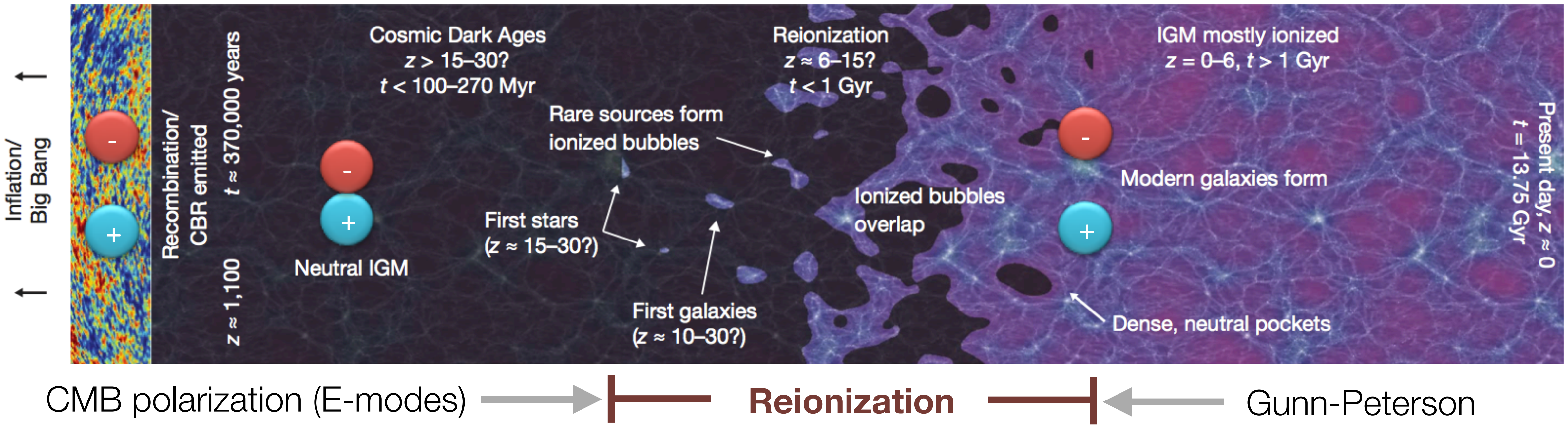

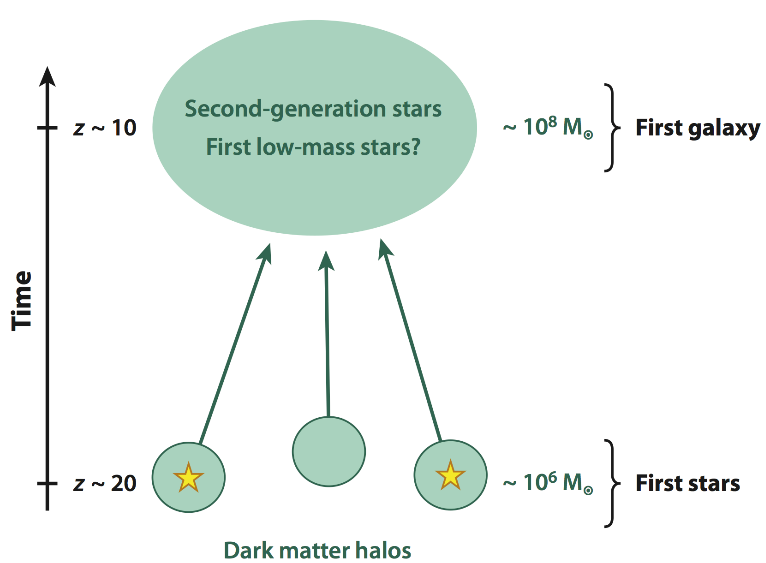

Bromm & Yoshida al. 2011

Universe has been re-ionized between z~15 and z~8

How and when did the first galaxies form?

Where they responsible for the re-ionization of the universe?

COSMIC TELESCOPES

Some of the most distant sources where discovered using cosmic telescopes (Zheng et al., 2012, z~9.6; Coe et al. 2013, z~10.8)

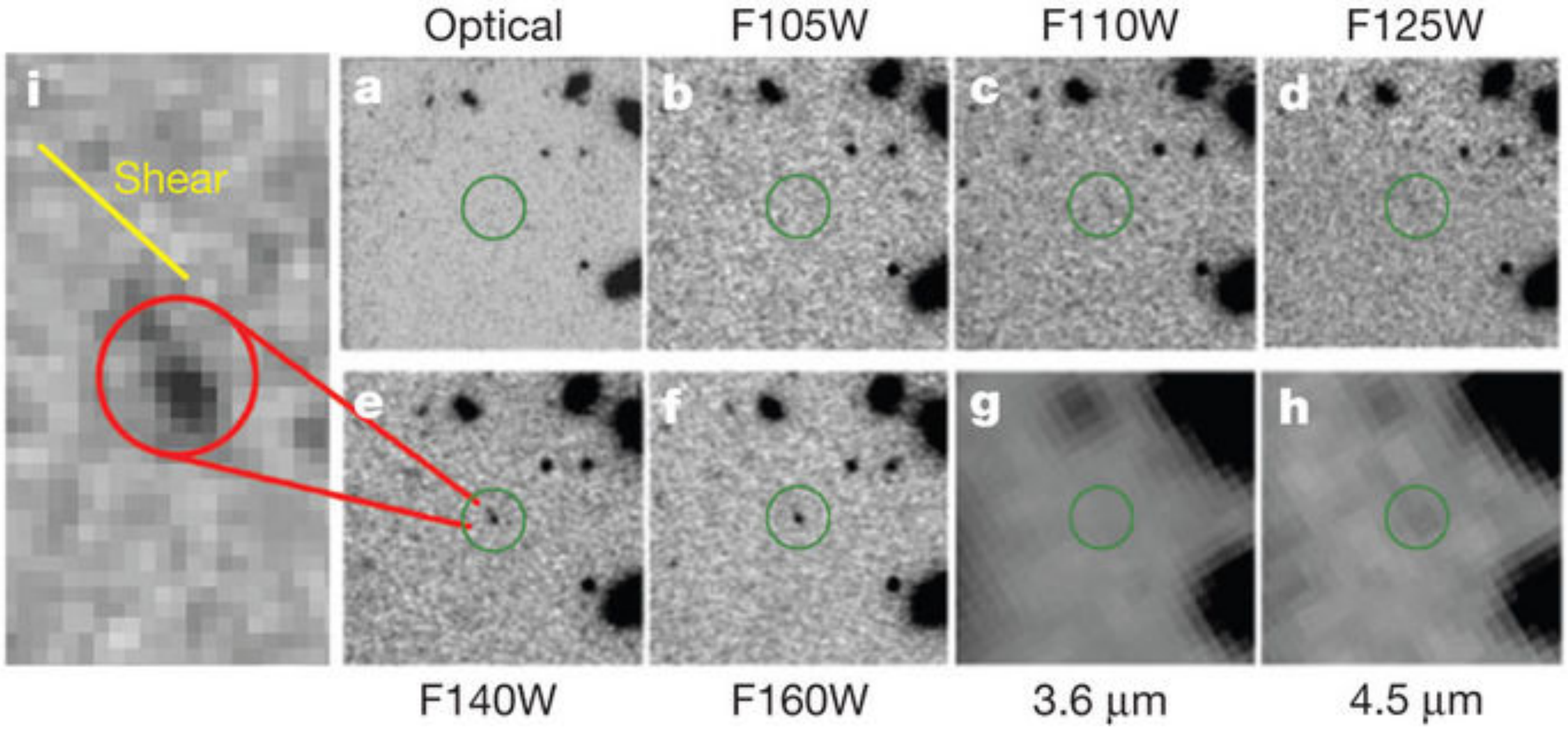

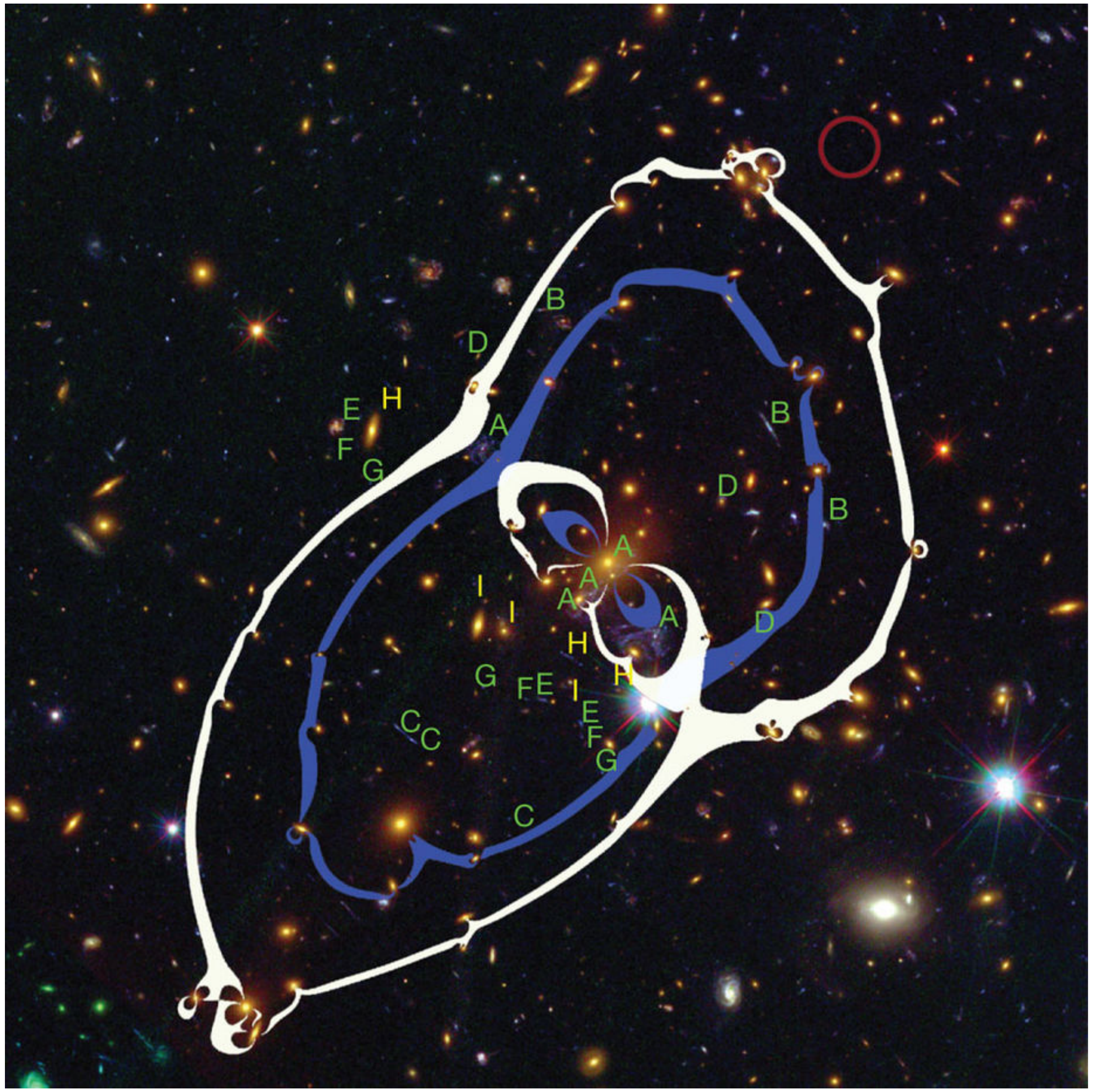

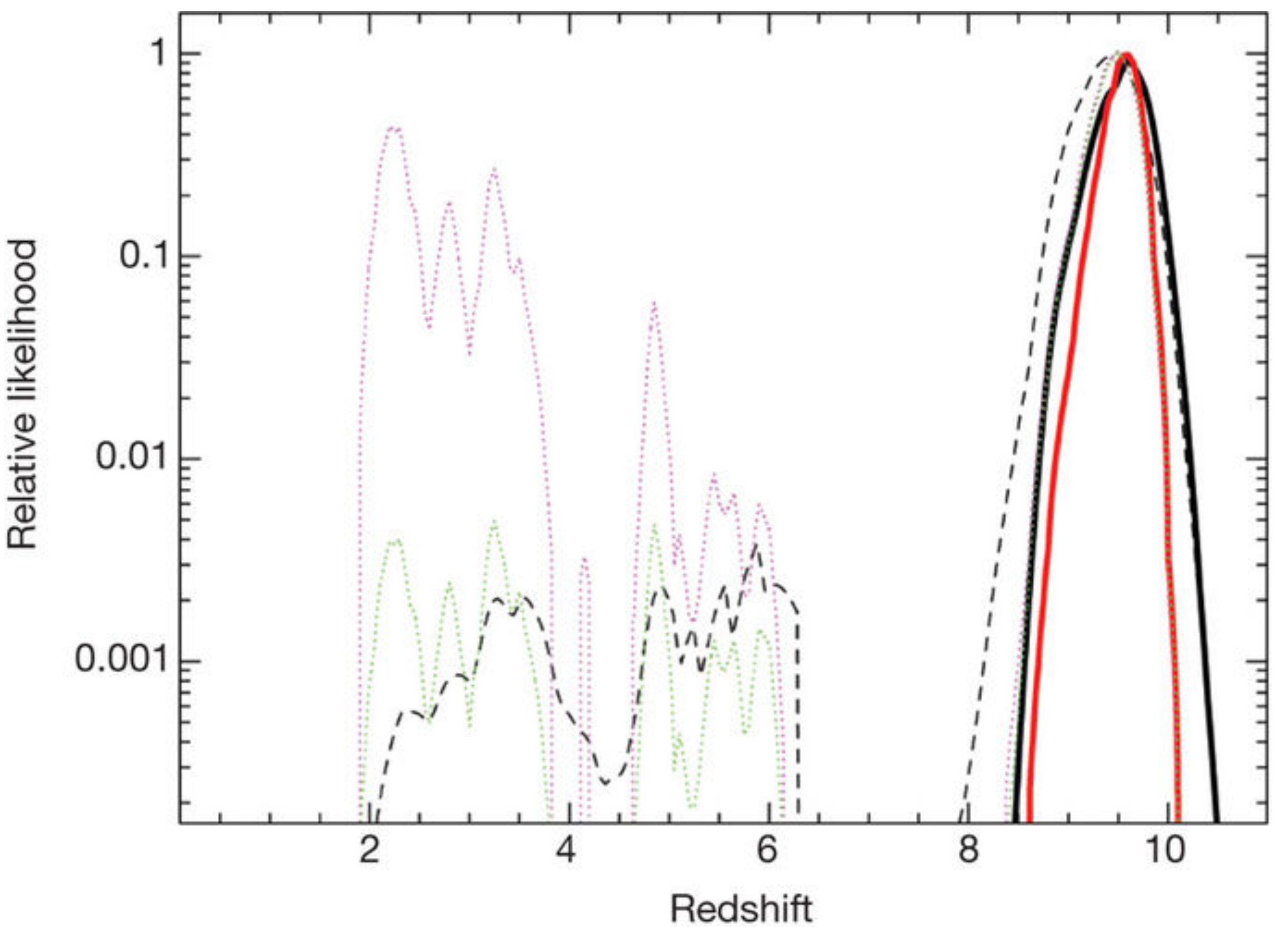

COSMIC TELESCOPES

Hashimoto et al. (2018) confirmed that the source is at z=9.1 using ALMA!

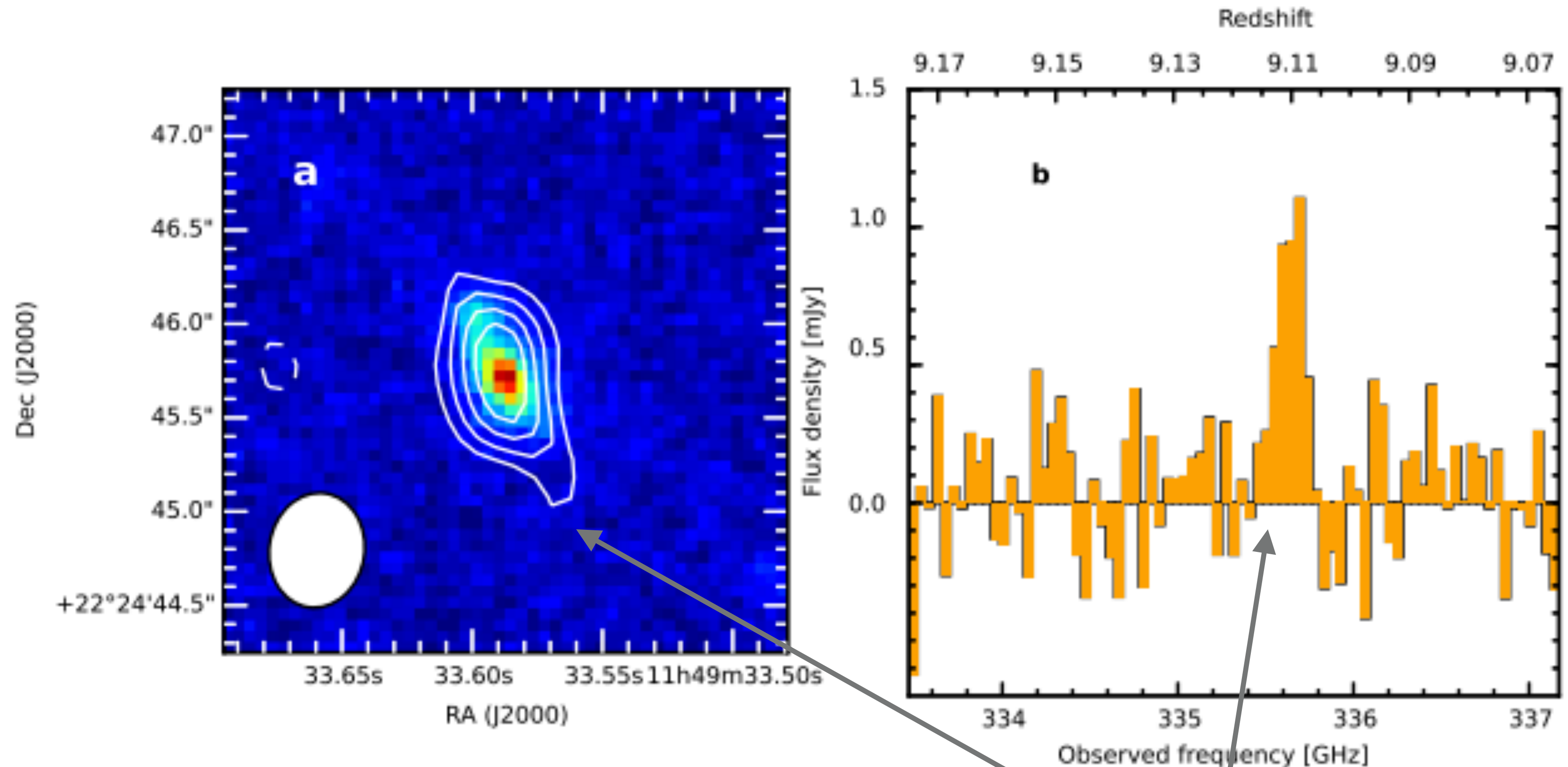

[OIII] 88μm emission

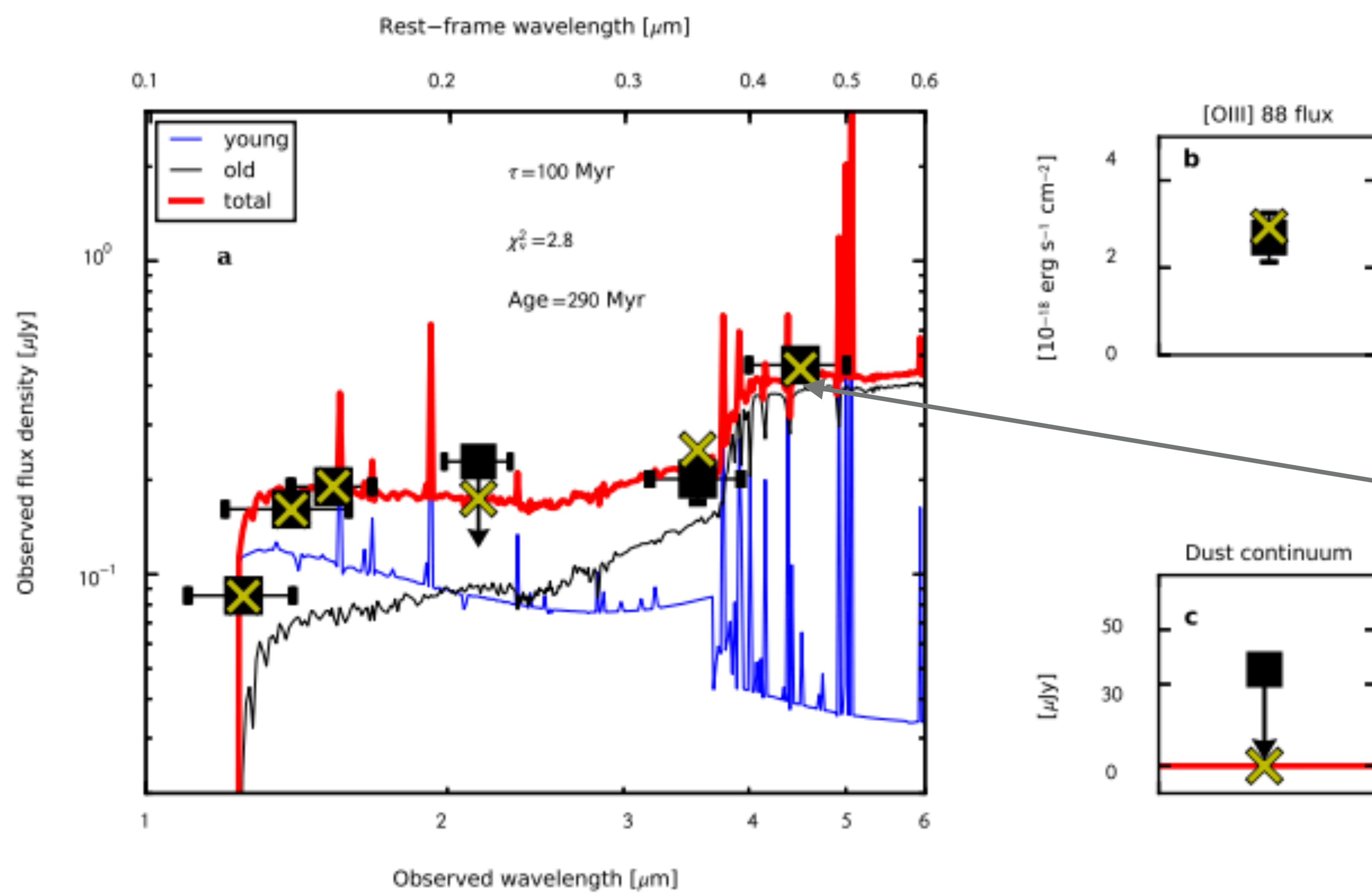

birth of the galaxy at z~15

COSMIC TELESCOPES

- problems: need to build very robust lens models to characterize these sources [luminosity, size, mass, SFR, LF,…]
- Sampled volume is very small

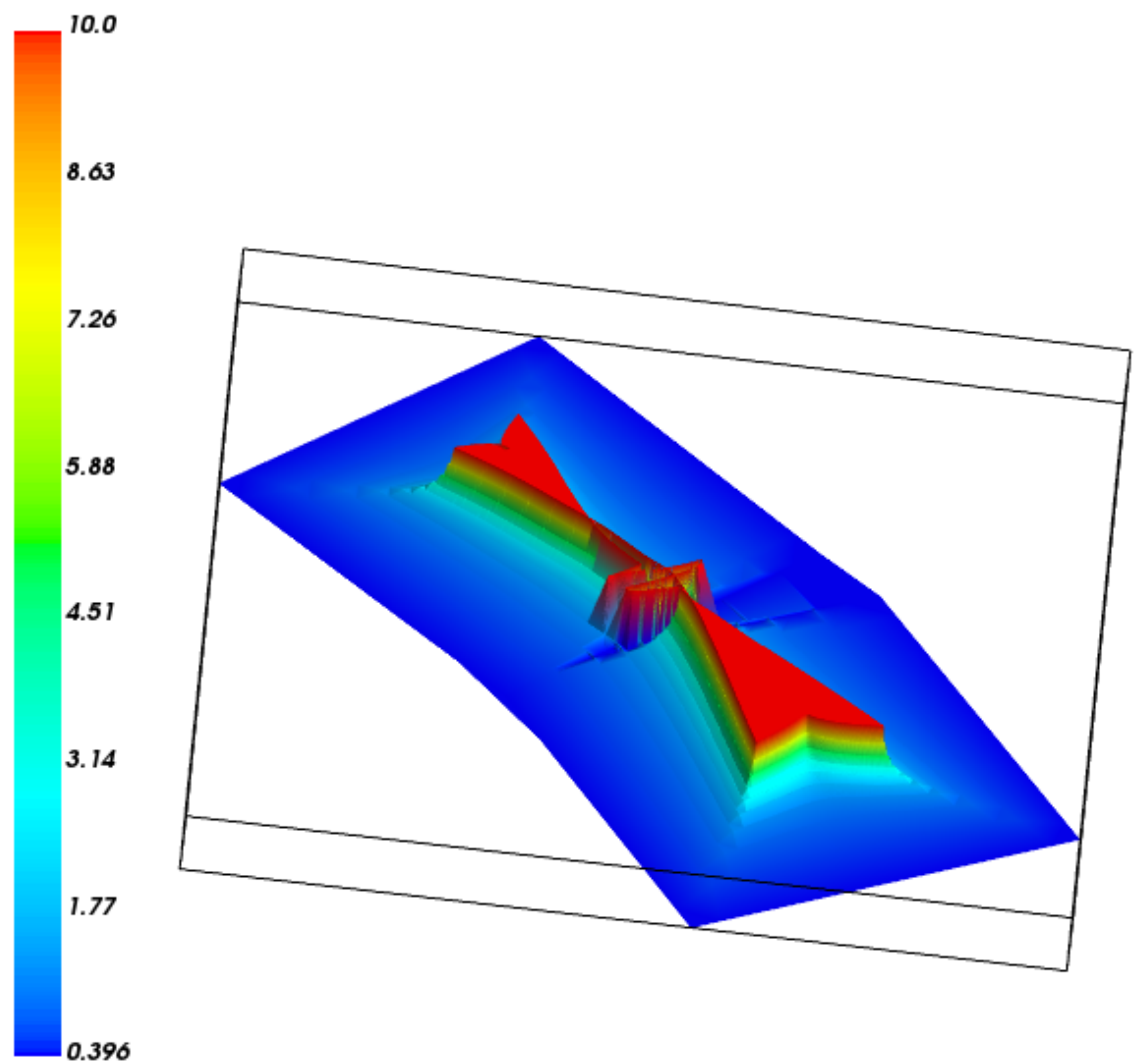

WEAK LENSING BY GALAXY CLUSTERS

Weak Lensing:
in short, “when we don’t see any evident distortion”

WEAK LENSES OR LARGE DISTANCES FROM STRONG LENSES

WEAK LENSES OR LARGE DISTANCES FROM STRONG LENSES

WEAK LENSES OR LARG

WHY MEASURING WEAK LENSING AROUND CLUSTERS?

- predictions of CDM: NFW profile, concentration mass relation, shapes of dark matter halos
- nature of DM: probe the non-collisional nature of DM particles e.g. by mapping DM and baryons
- cosmology: measure cluster masses out to the virial radius, build the cluster mass function, whose shape and evolution is extremely sensitive to cosmological parameters such as σ_8, Ω_M, w
- baryon-DM inter

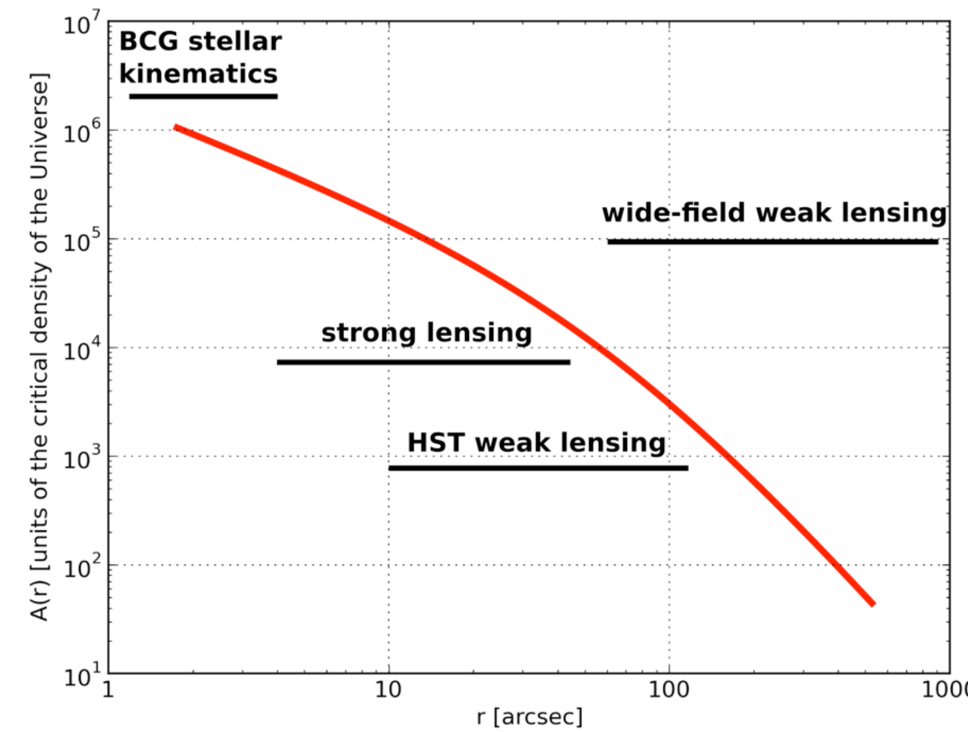

WHY MEASURING WEAK LENSING AROUND CLUSTERS?

- predictions of CDM: NFW profile, concentration mass relation, shapes of dark matter halos
- nature of DM: probe the non-collisional nature of DM particles e.g. by mapping DM and baryons
- cosmology: measure cluster masses out to the virial radius, build the cluster mass function, whose shape and evolution is extremely sensitive to cosmological parameters such as σ_8, Ω_M, w
- baryon-DM inter

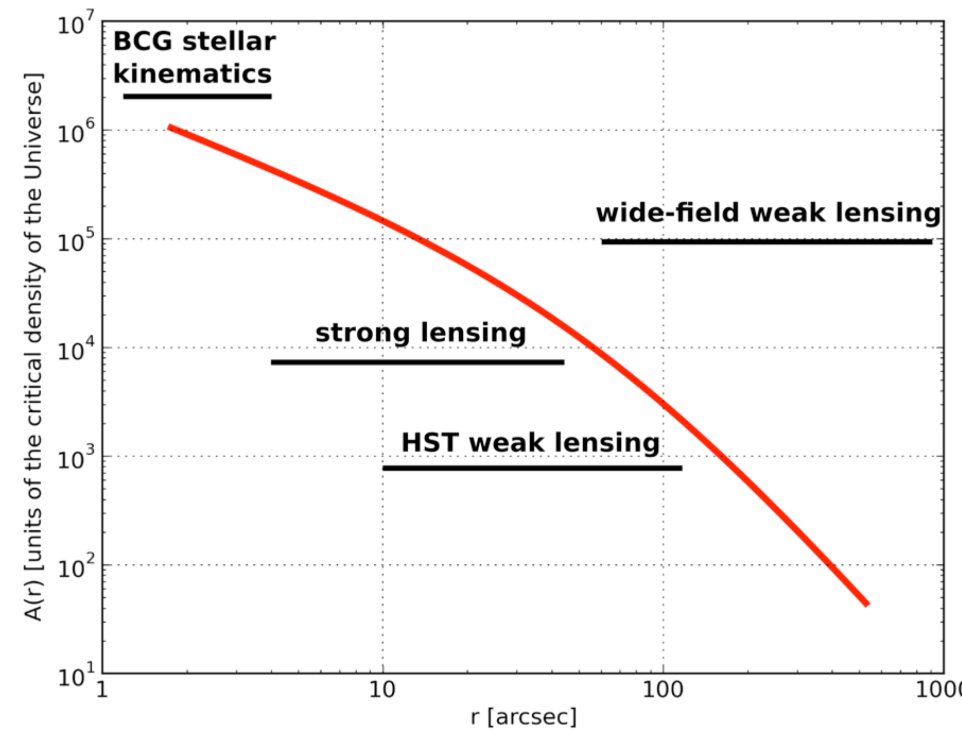

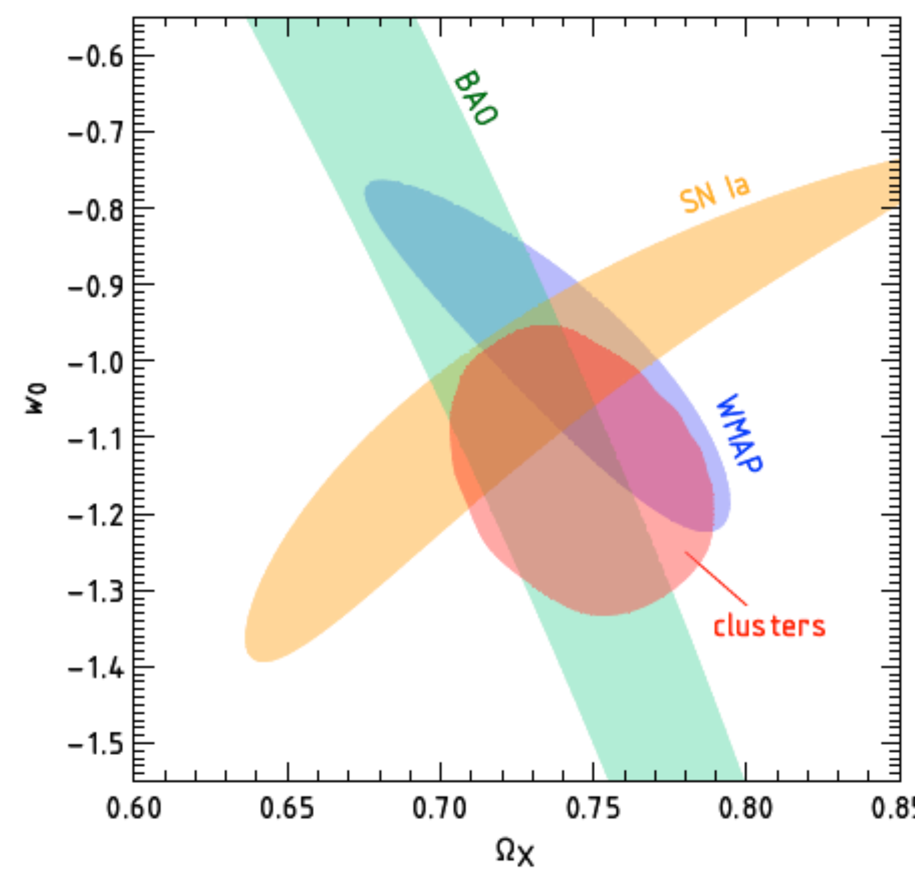

THE WEAK LENSING REGIME

- *κ and γ are small and nearly constant over the scale of a galaxy*
- *Circular sources are mapped into elliptical images*
- *If galaxies were circles, we would be able to measure the reduced shear from the image axis ratio and the orientation of the major axis*

$$\boldsymbol{\beta} - \boldsymbol{\beta}_0 = \mathcal{A}(\boldsymbol{\theta}_0) \cdot (\boldsymbol{\theta} - \boldsymbol{\theta}_0)$$

$$\mathcal{A}(\boldsymbol{\theta}) = (1-\kappa) \begin{pmatrix} 1 - g_1 & -g_2 \\ -g_2 & 1 + g_1 \end{pmatrix}$$

$$g(\boldsymbol{\theta}) = \frac{\gamma(\boldsymbol{\theta})}{[1 - \kappa(\boldsymbol{\theta})]}$$

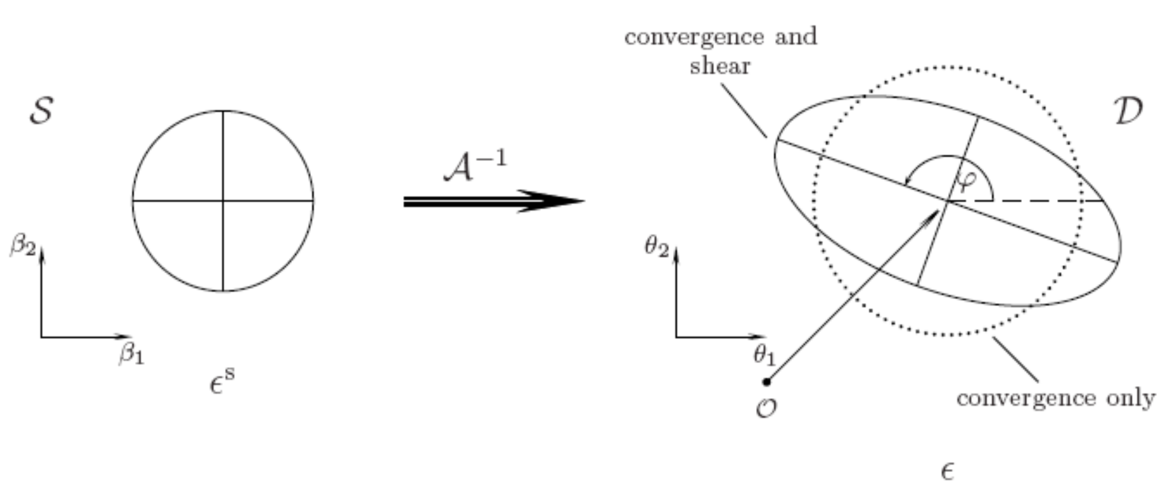

$$a = \frac{r}{1 - \kappa - \gamma} \quad , \quad b = \frac{r}{1 - \kappa + \gamma}$$

$$\epsilon = \frac{a-b}{a+b} = \frac{2\gamma}{2(1-\kappa)} = \frac{\gamma}{1-\kappa} \approx \gamma$$

$$|g| = \frac{1 - b/a}{1 + b/a} \quad \Leftrightarrow \quad \frac{b}{a} = \frac{1 - |g|}{1 + |g|}$$

WHAT IS THE IMAGE ELLIPTICITY?

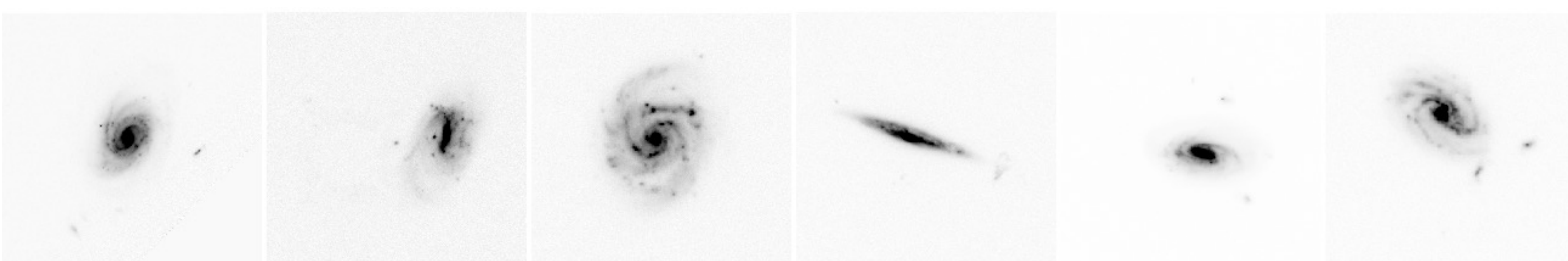

ELLIPTICITY FROM BRIGHTNESS MOMENTS

Observable: brightness distribution

Image centroid $\bar{\boldsymbol{\theta}} \equiv \frac{\int \mathrm{d}^2\theta \, I(\boldsymbol{\theta}) \, q_I[I(\boldsymbol{\theta})] \, \boldsymbol{\theta}}{\int \mathrm{d}^2\theta \, I(\boldsymbol{\theta}) \, q_I[I(\boldsymbol{\theta})]}$

Weight function $q_I(I) = \mathrm{H}(I - I_{\mathrm{th}})$;

Define a tensor of second order brightness moments:

$$Q_{ij} = \frac{\int \mathrm{d}^2\theta \, I(\boldsymbol{\theta}) \, q_I[I(\boldsymbol{\theta})] \, (\theta_i - \bar{\theta}_i) \, (\theta_j - \bar{\theta}_j)}{\int \mathrm{d}^2\theta \, I(\boldsymbol{\theta}) \, q_I[I(\boldsymbol{\theta})]} , \quad i, j \in \{1, 2\}$$

For an image with circular isophotes, $Q_{11}=Q_{22}$ *and* $Q_{12}=Q_{21}=0$

The trace of the Q describes the size of the image

ELLIPTICITY FROM BRIGHTNESS MOMENTS

Observable: brightness distribution

Image centroid $\bar{\boldsymbol{\theta}} \equiv \frac{\int \mathrm{d}^2\theta \, I(\boldsymbol{\theta}) \, q_I[I(\boldsymbol{\theta})] \, \boldsymbol{\theta}}{\int \mathrm{d}^2\theta \, I(\boldsymbol{\theta}) \, q_I[I(\boldsymbol{\theta})]}$

Weight function $q_I(I) = \mathrm{H}(I - I_{\mathrm{th}})$,

Define a tensor of second order brightness moments:

$$Q_{ij} = \frac{\int \mathrm{d}^2\theta \, I(\boldsymbol{\theta}) \, q_I[I(\boldsymbol{\theta})] \, (\theta_i - \bar{\theta}_i) \, (\theta_j - \bar{\theta}_j)}{\int \mathrm{d}^2\theta \, I(\boldsymbol{\theta}) \, q_I[I(\boldsymbol{\theta})]} \,, \quad i, j \in \{1, 2\}$$

For an image with circular isophotes, $Q_{11}=Q_{22}$ *and* $Q_{12}=Q_{21}=0$

The trace of the Q describes the size of the image

ELLIPTICITY FROM BRIGHTNESS MOMENTS

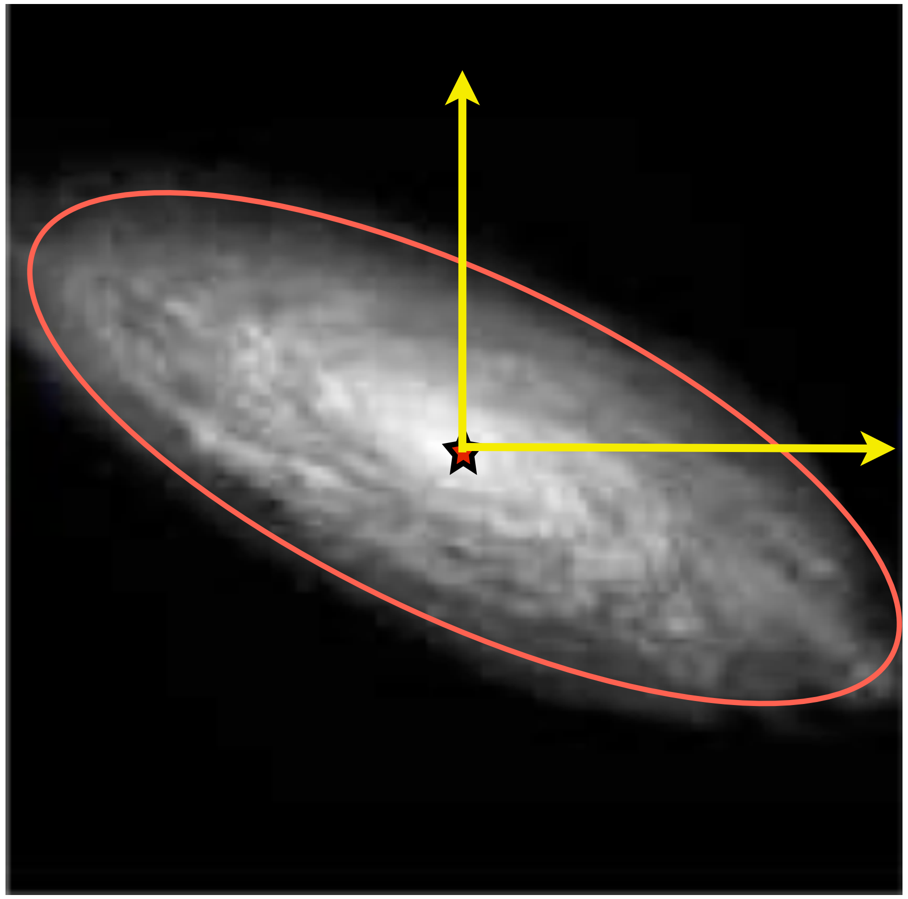

Observable: brightness distribution

Image centroid $\bar{\boldsymbol{\theta}} \equiv \frac{\int \mathrm{d}^2\theta\, I(\boldsymbol{\theta})\, q_I[I(\boldsymbol{\theta})]\, \boldsymbol{\theta}}{\int \mathrm{d}^2\theta\, I(\boldsymbol{\theta})\, q_I[I(\boldsymbol{\theta})]}$

Weight function $q_I(I) = \mathrm{H}(I - I_{\mathrm{th}})$

Define a tensor of second order brightness moments:

$$Q_{ij} = \frac{\int \mathrm{d}^2\theta\, I(\boldsymbol{\theta})\, q_I[I(\boldsymbol{\theta})]\, (\theta_i - \bar{\theta}_i)\, (\theta_j - \bar{\theta}_j)}{\int \mathrm{d}^2\theta\, I(\boldsymbol{\theta})\, q_I[I(\boldsymbol{\theta})]}\,, \quad i, j \in \{1, 2\}$$

For an image with circular isophotes, $Q_{11}=Q_{22}$ *and* $Q_{12}=Q_{21}=0$

The trace of the Q describes the size of the image

COMPLEX ELLIPTICITY AND REDUCED SHEAR

From Q_{ij}, one can define the complex ellipticity:

1. *Diagonalize the matrix*
2. *Eigenvalues give the inverse square root of the semi-axes*
3. *Eigenvectors give the direction*
4. *Take the two components along the θ_1 and θ_2 axes*

$$\epsilon \equiv \frac{Q_{11} - Q_{22} + 2\mathrm{i}Q_{12}}{Q_{11} + Q_{22} + 2(Q_{11}Q_{22} - Q_{12}^2)^{1/2}}$$

Note that we have used the complex notation introduced previously:

$$g = \frac{\gamma}{1-\kappa} = g_1 + ig_2 = |g|e^{2i\phi}$$

$$\epsilon = \epsilon_1 + i\epsilon_2 = |\epsilon|e^{2i\phi}$$

Thus, the ellipticity is not a scalar! It has a phase!

UNFORTUNATELY GALAXIES ARE NOT CIRCULAR…

$I_s(\vec{\beta})$ 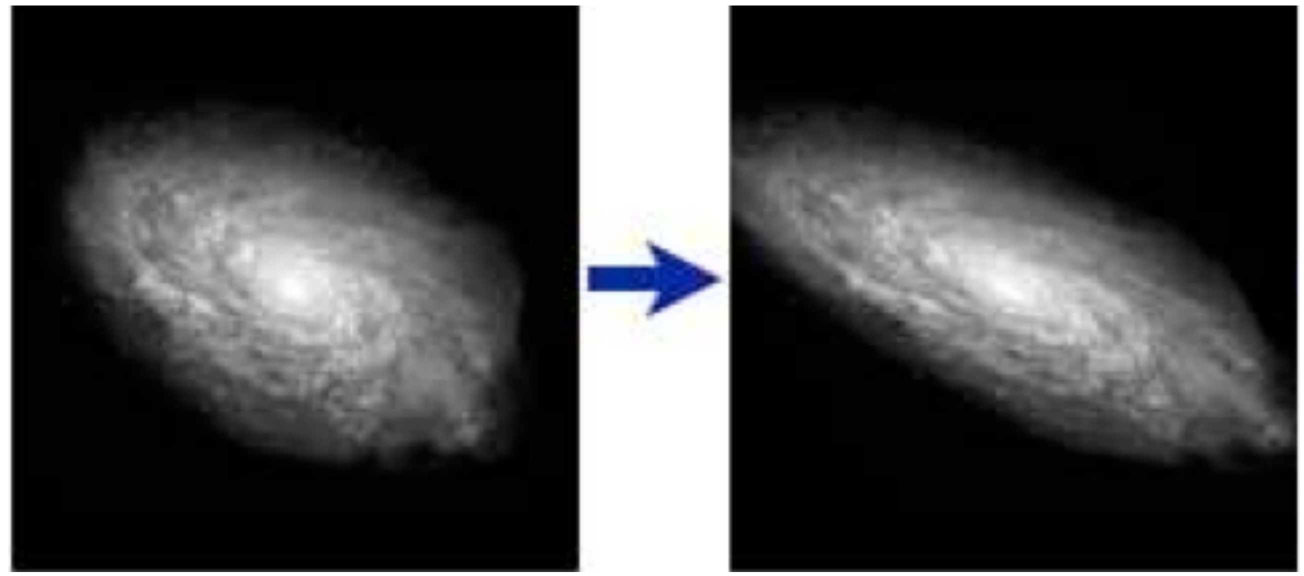 $I(\vec{\theta})$

We can use the lens mapping (at first order) to find the transformation between observed and intrinsic ellipticity

$$Q_{ij}^{(\mathrm{s})} = \frac{\int \mathrm{d}^2\beta\, q_I[I^{(\mathrm{s})}(\boldsymbol{\beta})]\, I\, (\beta_i - \bar{\beta}_i)\,(\beta_j - \bar{\beta}_j)}{\int \mathrm{d}^2\beta\, q_I[I^{(\mathrm{s})}(\boldsymbol{\beta})]\, I}\,, \quad i,j \in \{1,2\}$$

With $\quad \boldsymbol{\beta} - \bar{\boldsymbol{\beta}} = \mathcal{A}\,(\boldsymbol{\theta} - \bar{\boldsymbol{\theta}}) \qquad \mathrm{d}^2\beta = \det \mathcal{A}\, \mathrm{d}^2\theta,$

we find that $\quad Q^{(\mathrm{s})} = \mathcal{A}\, Q\, \mathcal{A}^T = \mathcal{A}\, Q\, \mathcal{A} \qquad \mathcal{A} \equiv \mathcal{A}(\bar{\boldsymbol{\theta}})$

$$\mathcal{A}(\boldsymbol{\theta}) = (1-\kappa)\begin{pmatrix} 1-g_1 & -g_2 \\ -g_2 & 1+g_1 \end{pmatrix} \qquad \epsilon \equiv \frac{Q_{11} - Q_{22} + 2\mathrm{i}Q_{12}}{Q_{11} + Q_{22} + 2(Q_{11}Q_{22} - Q_{12}^2)^{1/2}} \qquad \epsilon^{(\mathrm{s})} = \begin{cases} \dfrac{\epsilon - g}{1 - g^*\epsilon} & \text{if } |g| \le 1\,; \\[2ex] \dfrac{1 - g\epsilon^*}{\epsilon^* - g^*} & \text{if } |g| > 1\,. \end{cases}$$

UNFORTUNATELY GALAXIES ARE NOT CIRCULAR…

Using the fact that $\mathcal{A}(\boldsymbol{\theta}) = (1-\kappa)\begin{pmatrix} 1-g_1 & -g_2 \\ -g_2 & 1+g_1 \end{pmatrix}$

and that $\epsilon \equiv \dfrac{Q_{11} - Q_{22} + 2\mathrm{i}Q_{12}}{Q_{11} + Q_{22} + 2(Q_{11}Q_{22} - Q_{12}^2)^{1/2}}$

we can show that $Q^{(\mathrm{s})} = \mathcal{A}\, Q\, \mathcal{A}^T = \mathcal{A}\, Q\, \mathcal{A}$ *implies*

$$\epsilon^{(\mathrm{s})} = \begin{cases} \dfrac{\epsilon - g}{1 - g^* \epsilon} & \text{if } |g| \le 1 \; ; \\ \\ \dfrac{1 - g\epsilon^*}{\epsilon^* - g^*} & \text{if } |g| > 1 \; . \end{cases}$$

ESTIMATING THE REDUCED SHEAR

We assume that the intrinsic orientations of galaxies (phases of the complex ellipticity) are random. In this case,

$$E(\epsilon^{(s)}) = 0$$

$$\epsilon^{(\mathrm{s})} = \begin{cases} \dfrac{\epsilon - g}{1 - g^* \epsilon} & \text{if } |g| \le 1\ ; \\[2ex] \dfrac{1 - g\epsilon^*}{\epsilon^* - g^*} & \text{if } |g| > 1\ . \end{cases} \quad \Rightarrow \quad \mathrm{E}(\epsilon) = \begin{cases} g & \text{if } |g| \le 1 \\ 1/g^* & \text{if } |g| > 1 \end{cases}$$

Each image ellipticity provides an un-biased estimate of the local shear. However this is very noisy. The noise is determined by the intrinsic ellipticity dispersion

$$\sigma_\epsilon = \sqrt{\left\langle \epsilon^{(\mathrm{s})} \epsilon^{(\mathrm{s})*} \right\rangle}$$

Noise can be beaten down by averaging over many galaxy images. The accuracy of the shear estimate depends on the local density of galaxies for which shape can be measured. Thus, deep imaging observations are required.

$$\gamma \approx g \approx \langle \epsilon \rangle$$

CHALLENGES

- images are blurred by instrument **PSF** and by the atmosphere. PSF tends to circularize shapes but can also introduce artificial elongations, i.e. spurious signal
- images are **pixelated**
- sometimes galaxies are **blended**
- in the case of shear measurements from space (HST), the "breathing" of the telescope causes PSF variations
- several **instrumental effects** can mimic as shear signal (e.g. CTE, bad tracking, star saturations, ghosts, cosmic rays)
- if there are **intrinsic alignments**, then the shear measurement will be biased
- lensing signal (shear) is **redshift** dependent. This needs to be taken into account, especially when dealing with deep observations
- only galaxies behind the lens (cluster) are lensed. Averaging over galaxies that are erroneously classified as background but in fact are in the cluster foreground or within the cluster causes **signal dilution**
- and more…

KSB SCHEME

- designed to correct the ellipticity measurements from PSF anisotropy
- suppose this has a complex ellipticity ***q***. This can be measured from stars in the FOV and then fitted using a low-order polynomial
- assume the shear and the PSF anisotropy are small. Then their effect can be assumed to be linear:

$$\epsilon_\alpha^{obs} = \epsilon_\alpha^0 + P_{\alpha\beta}^{\mathrm{sm}} q_\beta + P_{\alpha\beta}^{g} g_\beta$$

observed ellipticity

true ellipticity

response of the image ellipticity to the shear

response of the image ellipticity to the PSF anisotropy

KSB SCHEME

$$\epsilon_\alpha^{obs} = \epsilon_\alpha^0 + P_{\alpha\beta}^{\rm sm} q_\beta + P_{\alpha\beta}^g g_\beta$$

averaging $$\epsilon = \left(P^g\right)^{-1} \left(\epsilon^{obs} - P^{\rm sm} q\right)$$

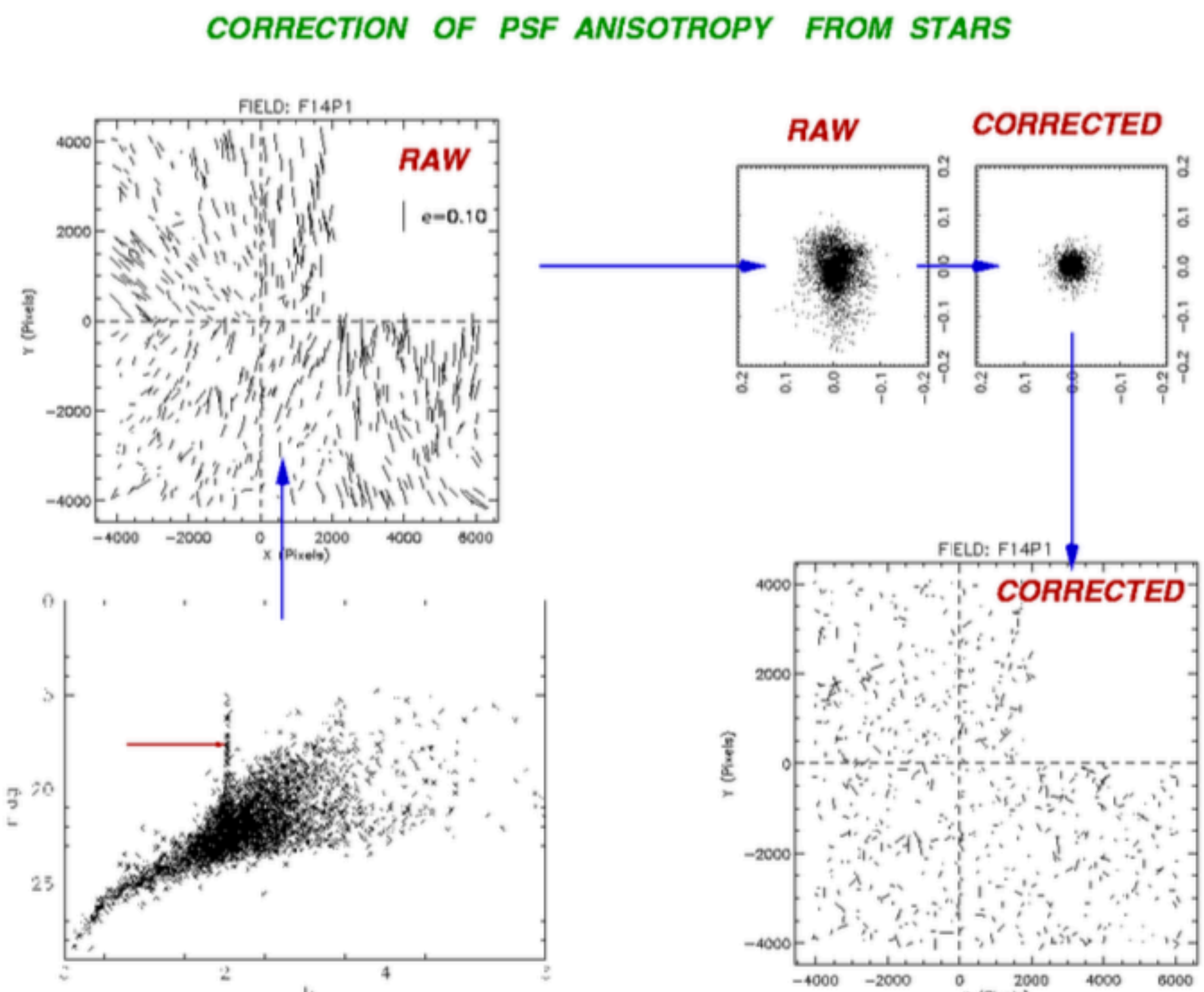

P. Schneider